20m Africa Rice Distribution Map of 2023

Jingling Jiang [1,2,3], Hong Zhang [2,1,3], Ji Ge [1,2,3], Lijun Zuo[1], Lu Xu [1,2], Mingyang Song [1,2,3], Yinhaibin Ding[1,2,3], Yazhe Xie [1,2,3], Wenjiang Huang[1,3]

[1]Key Laboratory of Digital Earth Science, Aerospace Information Research Institute, Chinese Academy of Sciences, Beijing 100094, China;
[2]International Research Center of Big Data for Sustainable Development Goals, Beijing 100049, China
[3]College of Resources and Environment, University of Chinese Academy of Sciences, Beijing 100049, China

Correspondence to: Hong Zhang (zhanghong@radi.ac.cn)

Abstract. In recent years, the demand for rice in Africa has been growing rapidly, and in order to meet this demand, the rice cultivation area is also expanding rapidly, thus it is of great significance to monitor the rice cultivation in Africa. The spatial and temporal distribution of rice cultivation in Africa is complex, making it difficult to use phenology-based rice identification methods, and the existing rice distribution products of Africa are all grid-based statistical data with low resolution, unable to obtain accurate rice field location and available labels. To address these two difficulties, based on time-series optical and dual-polarisation Synthetic Aperture Radar (SAR) data, this study proposes a sample set construction method by fast coarse positioning assisted visual interpretation, and a feature importance guided supervised classification combining multiple temporal optical and SAR features to reduce the impact of rice diversity in Africa. Firstly, we use the time-series statistical features of VH data for fast coarse positioning and screening of possible rice areas, and combine multiple auxiliary data for visual interpretation to construct the sample set; secondly, based on the complementary information in SAR data and optical data, the 20 meter Africa rice distribution map of 2023 was completed by combining the object-oriented segmentation results of temporal optical images and the pixel-based classification results of temporal SAR data features after feature selection. The average classification accuracy of the proposed method on the validation set is more than 85%, and the R^2 of the linear fit to various existing statistical data is more than 0.9, which proves that the proposed method can achieve the spatial distribution mapping of rice under the complex climatic conditions in a large region, providing crucial data support for rice monitoring and agricultural policy development. The dataset is available at https://doi.org/10.5281/zenodo.13729353 (Jiang et al., 2024).

1 Introduction

Rice is the staple food for half of the world's population (Kuenzer and Knauer, 2013), providing over a quarter of the calories for approximately half of the population (Wu et al., 2022), playing an important role in maintaining global food security and also crucial to the economies of many developing countries (Seck et al., 2012; Ajala and Gana, 2015). In 2021, rice accounted for approximately 8.3% of the world's major crop production (Fao, 2023). In Africa, rice accounted for approximately 3.8% of the main crop yield and 4.7% of the global rice production. Despite its current modest share, the demand

for rice in sub-Saharan Africa is increasing at over 6% annually due to population growth, urbanization, and changes in consumer preferences, surpassing any other staple food (Arouna et al., 2021). In order to meet the higher demand for rice, the synchronous growth of local rice production and imports in Africa, and the expansion of rice area rather than the increase in production, are the main driving forces for the increase in domestic production. In the past thirty years, the cultivated land area has expanded by about 400,000 hectares per year (Yuan et al., 2024).

In 2023, in order to promote food and nutrition security in Africa, the African Rice Center proposed the 2030 Africa Rice Research and Innovation Strategy (Africarice, 2023) to transform the rice-based agricultural food system, and the rice area in Africa will continue to grow. Meanwhile, rice cultivation and production are important sources of income for a large number of African households (Hussain et al., 2020). However, rice cultivation in Africa also faces many challenges. Firstly, Africa is highly susceptible to the impacts of climate change, such as extreme weather events, changes in precipitation patterns, and rising temperatures, which can have a significant impact on agricultural production (Field and Barros, 2014; Ogisi and Begho, 2023). Land use changes across Africa, particularly urban expansion and deforestation, also influence the distribution of rice cultivation areas (Lambin and Geist 2008, Bren d'Amour, Reitsma et al. 2017). Consequently, it is essential to obtain high-resolution maps of rice spatial distribution in Africa for monitoring the condition of rice cultivation across the continent.

In recent years, the global crop mapping datasets that include rice in Africa mainly include SPAM2010 (Yu et al., 2020), GAEZ+2015 (Global Agro Ecological Zones) (Frolking et al., 2020), SPAMAF2017 (International Food Policy Research, 2020), and CROPGRIDS (Tang et al., 2023). SPAM2010 and SPAMAF2017 datasets are based on the SPAM model (Spatial Production Allocation Model) developed by the International Food Policy Research Institute (IFPRI), which utilizes geographic spatial data such as land use types and crop statistical data as inputs to make reasonable estimates of crop distribution within the decomposed units using a cross entropy approach, with a spatial resolution of 5 minite (~10km). GAEZ+2015 utilized the GAEZ model and FAO's crop statistical data to generate grid distribution products for 26 crops, with a spatial resolution of 5 minite (~10km). CROPGRIDS has generated the latest global georeferenced dataset of 173 crops using 26 published grid datasets, with a spatial resolution of 0.05° (~5.5km). The existing datasets have low resolution and are all gridded datasets rather than high resolution distribution maps. Moreover, these data is generally outdated, making them of limited significance for monitoring rice cultivation in Africa.

Due to the complementarity of information between SAR data and optical remote sensing data, current large-scale rice mapping benefits from multi-source data that combines SAR data and optical remote sensing data as data sources (Han et al., 2021; Shen et al., 2023; Ginting et al., 2024). Current rice mapping methods are usually divided into: 1) Phenology-based classification methods. For example, Qiu (Qiu et al., 2015) utilized the CCVS (the Combined Consideration of Vegetation phenology and Surface water variations) index, constructed using the Land Surface Water Index (LSWI) and Enhanced Vegetation Index (EVI) during the rice heading and transplanting stages, to map rice in the complex terrain of southern China. Similarly, Zhang (Zhang et al., 2023) employed the SPRI (SAR-based Rice Mapping Index) index, which describes the growth status from the transplanting to maturity stages, to achieve sample-free mapping of double-cropping rice. These methods do

not require sample data but rely heavily on accurate phenological information. 2) Methods leveraging time-series curve

65 similarity measures, such as DTW (Dynamic Time Warping) (Guan et al., 2016) and its improved version TWDTW (Time Weighted Dynamic Time Warping) (Singh et al., 2021; Tian et al., 2024), requiring only a small number of rice samples to obtain a standard rice growth curve; 3) Supervised classification methods, including various machine learning methods (Wang et al., 2020; Zhang et al., 2020; You et al., 2021a) and rapidly developing deep learning methods in recent years (Zhu et al., 2021; Sun et al., 2023). These methods offer several advantages for rice mapping. They do not require phenological

70 information, making them adaptable to different regions and growing conditions. Additionally, they provide high classification accuracy and robustness when large amounts of labeled sample data are available. This allows for more precise identification and mapping of rice fields, even in complex landscapes or where other methods struggle. However, the effectiveness of these approaches depends on the availability and quality of the training data.

The first challenge in mapping rice in Africa lies in the significant temporal and spatial variability of rice cultivation due to its

75 tropical and subtropical climate, as illustrated in Fig. 1. The data in this figure is derived from the rice calendar product RiceAtlas (Laborte et al., 2017) published in 2017, annotating the months when the main and secondary seasons of rice planting in Africa end and harvest begins. African rice cultivation includes both single and double cropping systems, with variations in planting times and growth durations across different seasons. This makes it difficult to apply a uniform phenological description for mapping rice across the entire continent. Notably, large areas of rainfed rice cultivation (Balasubramanian et

80 al., 2007) in Africa lack the distinct flooding signals typical of irrigated rice, which are commonly used in widely adopted rice mapping methods that rely on detecting flooding periods (Guo et al., 2019; Zhan et al., 2021; Wei et al., 2022). Consequently, phenology-based rice mapping methods are challenging to apply in Africa. Similarly, DTW-based approaches are difficult to implement due to the variability in rice cropping intensity and phenology, which hinders the identification of a standard rice growth curve. Therefore, integrating time-series data with supervised classification emerges as the primary strategy for

85 mapping rice spatial distribution in Africa. However, the main challenge of this approach lies in constructing the sample set. Existing rice distribution products for Africa are grid-based, making it difficult to quickly identify rice-growing areas for sample set construction. Moreover, the diversity of rice cultivation in Africa—spanning phenology (including cropping intensity), farming practices (irrigated/rainfed), and environmental conditions (plains, hills)—complicates the identification of rice fields and makes it challenging to ensure the representativeness and completeness of the samples.
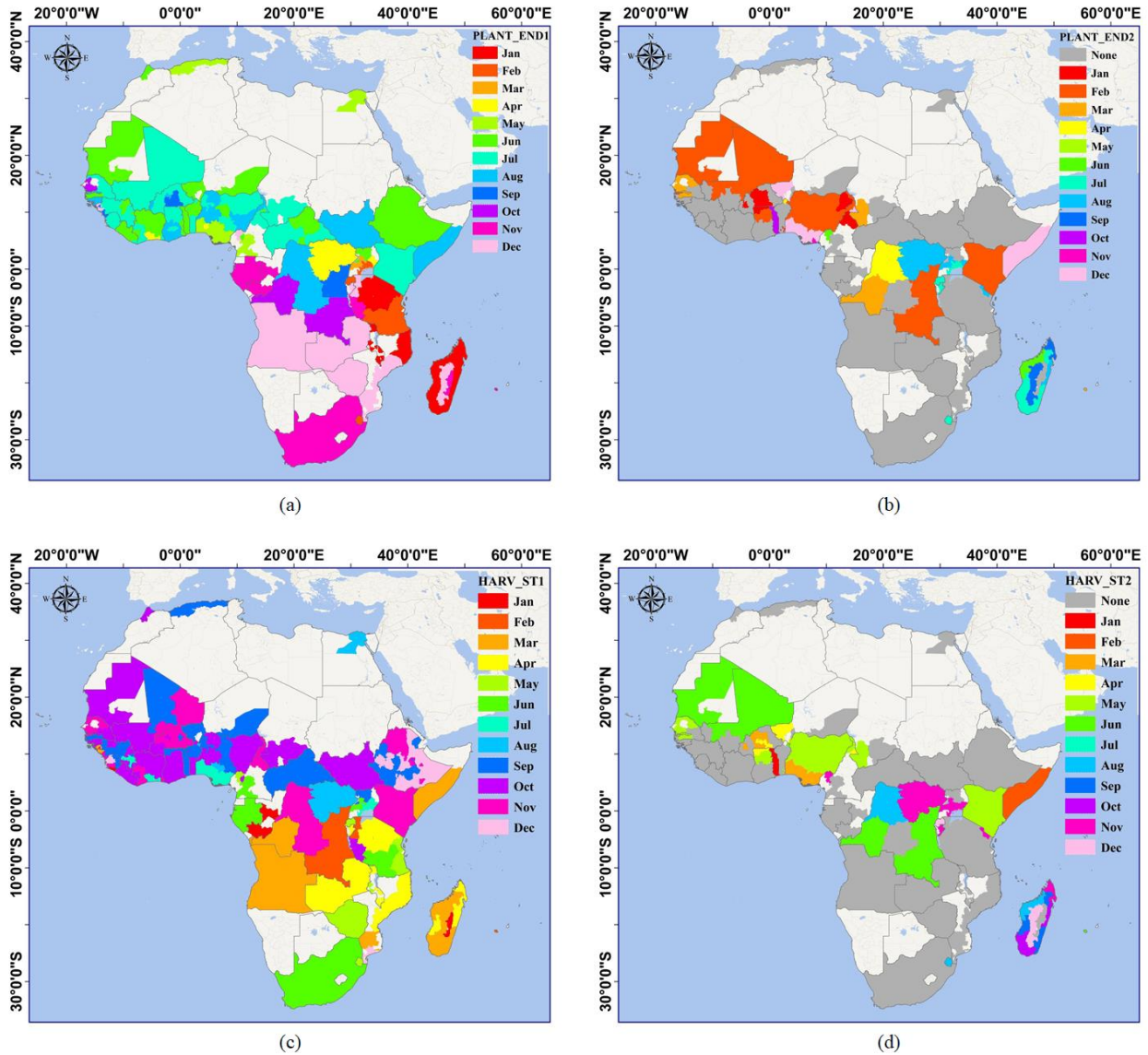
Figure 1. Rice planting calendar: (a) main rice season planting end date, (b) secondary rice season planting end date, (c) main rice season harvest start date, and (d) secondary rice season harvest start date. Data sourced from RiceAtlas.

In recent years, the Google Earth Engine (GEE) platform has provided robust support for high-resolution crop mapping. GEE integrates extensive remote sensing data and geographic information system tools, enabling rapid processing and analysis of massive time-series datasets (Gorelick et al., 2017). In particular, Sentinel satellite data (Sentinel-1 and Sentinel-2) have been widely applied in crop monitoring and mapping due to their high spatial resolution and frequent temporal coverage (Saad El Imanni et al., 2022; Waleed et al., 2022; Luo et al., 2023; Zoungrana et al., 2024). Additionally, the GEE platform supports

various supervised classification methods, including Random Forest (RF), Support Vector Machine (SVM), and Classification and Regression Trees (CART) (Liu et al., 2020; You et al., 2021b; Avcı et al., 2023). By integrating multi-source time-series Sentinel data with these supervised classification algorithms available on the GEE platform, it has become feasible to achieve large-scale, high-resolution, and high-accuracy mapping of rice distribution in Africa.

In summary, this study employs a multi-source time series data approach combined with classification algorithms to produce large-scale and high-resolution rice distribution maps across Africa. Specifically, to address the challenge of sample collection, time-series statistical features from Sentinel-1 VH data are used for fast coarse positioning of potential rice-planting areas, followed by visual interpretation using various auxiliary datasets to create reliable samples. During the classification stage, object-based segmentation results derived from Sentinel-2 optical time-series data are integrated with feature importance guided Random Forest classification results from Sentinel-1 SAR time-series to obtain more precise rice paddy boundaries and reduce noise in heterogeneous landscapes. This approach successfully generated a 20-meter resolution rice distribution map for Africa in 2023. The research could provide scientific support for rice management in Africa, contribute to improving rice yields, ensure food security, and offer data for addressing climate change. The findings are expected to be valuable for policymakers, agricultural scientists, and farmers alike.

2 Materials

2.1 Study site

In this study, 34 countries with harvested rice areas exceeding 5,000 hectares, as reported by FAO (Food and Agriculture Organization of the United Nations) statistics in 2022, were selected as the study regions for rice spatial distribution mapping (Fao, 2022), shown in Fig. 2. These include 3 countries in Northern Africa (Egypt, Morocco, Sudan), 15 countries in Western Africa (Benin, Burkina Faso, Côte d'Ivoire, Gambia, Ghana, Guinea, Guinea-Bissau, Liberia, Mali, Mauritania, Niger, Nigeria, Senegal, Sierra Leone, Togo), 5 countries in Central Africa (Angola, Cameroon, Central African Republic, Chad, Democratic Republic of the Congo), and 11 countries in Eastern Africa (Burundi, Ethiopia, Kenya, Madagascar, Malawi, Mozambique, Rwanda, South Sudan, Uganda, Tanzania, Zambia). The regional division follows the United Nations' Geoscheme (United Nations 2013).
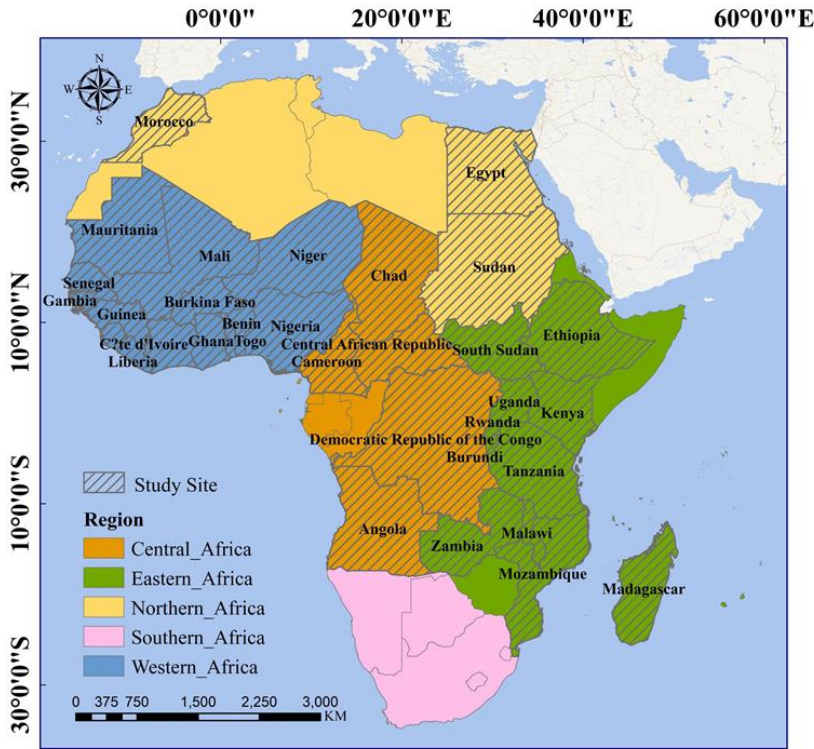
Figure 2. Study site: 34 countries in Africa with rice harvest areas exceeding 5000 hectares in 2022 according to FAO (diagonally marked area). GIS country boundaries in Figure 2 are available from GADM (https://gadm.org)

125 The climatic variations across different sub-regions of Africa result in diverse rice cultivation practices. In Northern Africa, dominated by desert and Mediterranean climates, the hot and arid conditions, coupled with scarce rainfall, limit rice cultivation to areas with stable water resources, such as the Nile River basin. Rice is primarily cultivated as a single-season crop, relying heavily on irrigation systems. In Western Africa, coastal regions experience tropical rainforest climates, while the interior regions have tropical savanna climates. Rainfall decreases progressively from the coast to inland, leading to rainfed rice

130 cultivation predominantly in coastal areas during the rainy season, which typically spans from May to October, allowing for single-season planting. In inland areas, rice cultivation often depends on flood irrigation or irrigation systems, enabling multi-season cropping. Central Africa also features a tropical rainforest and savanna climate but with uneven rainfall distribution across seasons. As a result, phenological patterns of rainfed rice vary widely in rainforest areas, while rice cultivation in savanna areas partly depends on seasonal flooding or irrigation. In Eastern Africa, the highland regions are characterized by

135 warm and humid mountain climates, where rice cultivation primarily relies on natural rainfall, with the main rainy seasons occurring from April to June and October to December. In contrast, lowland areas have tropical savanna climates, requiring irrigation support for rice cultivation.

2.2 Data source

2.2.1 Satellite data

140   The main data sources in the study are time-series SAR data and optical data for their high temporal and spatial coverage. Specifically, the monthly average VH and VV data of Sentinel-1 satellite for the whole year of 2023 were obtained as SAR data input on the GEE platform. Because rice is sensitive to NDWI (Normalized Difference Water Index) and NDVI (Normalized Difference Vegetation Index)(Zhang et al., 2019; De Lima et al., 2021), the monthly average B3, B4, B8, and B8A band data of Sentinel-2 satellite for the whole year of 2023 were obtained as optical data input to composite NDWI and

145   NDVI. The substantial volume of data, covering multiple spectral and temporal dimensions, enhances the model's capability to detect seasonal variations and accurately map rice fields in diverse agro-ecological zones across Africa. Table 1 presents the number of satellite images utilized for the monthly average composite across each country within the study site. A total of 29,722 Sentinel-1 (S1) images and 387,439 Sentinel-2 (S2) images were employed in the experiment.

Table 1. Number of satellite images used in the study

No.	Country	Number of S1 images	Number of S2 images	No.	Country	Number of S1 images	Number of S2 images
1	Angola	418	19765	18	Madagascar	1106	15324
2	Benin	365	2142	19	Malawi	441	3008
3	Burkina Faso	486	5126	20	Mali	1400	20949
4	Burundi	207	1126	21	Mauritania	1274	17083
5	Cameroon	1319	8253	22	Morocco	1448	8933
6	Central African Republic	963	9542	23	Mozambique	1877	26645
7	Chad	1139	19564	24	Niger	1565	18297
8	Côte d'Ivoire	514	5575	25	Nigeria	1677	14716
9	Democratic Republic of Congo	3762	55967	26	Rwanda	238	917
10	Egypt	1052	16529	27	Senegal	379	4192
11	Ethiopia	1625	17062	28	Sierra Leone	213	1872
12	Gambia	86	791	29	South Sudan	659	9882
13	Ghana	413	4407	30	Sudan	488	29213
14	Guinea	515	4704	31	Togo	120	1822
15	Guinea-Bissau	142	1233	32	Uganda	639	4534
16	Kenya	972	8917	33	United Republic of Tanzania	1427	14807
17	Liberia	245	2304	34	Zambia	548	12238

 2.2.2 Land cover data

During the sample set construction phase, cropland data from the European Space Agency's (ESA) WorldCover data for 2020 and 2021 were used as a reference. By integrating land cover data from two consecutive years, the study ensured better temporal consistency and reliability in sample selection. The use of this land cover data also facilitated the initial separation of rice and non-rice areas, supporting more precise training and validation in the subsequent classification processes.

 2.2.3 Rice Grid Data

During the sample set construction phase, rice grid data from the CROPGRIDS (Tang et al., 2023) grid distribution product released in 2023 was used as a reference.

2.2.4 Statistical data

Three kinds of statistical data were used in the study, as shown in Table 2.

 Table 2. Statistical data on rice area used in the study

Statistical Data	Data Time	Retrieve Time
USDA(United States Department of Agriculture): Rice planting/harvesting area in African countries **(Usda, 2023)**	2023	2024/02
FAO(Food and Agriculture Organization of the United Nations): Rice harvesting area in African countries **(Fao, 2022)**	2022	2024/03
CARD(COALITION for African Rice Development): Rice planting/harvesting area in CARD countries **(Card, 2022)**	2020/2021	2024/05

2.2.5 Administrative distribution data of rice planting intensity

In the comparison stage with statistical data, the administrative distribution data of rice planting intensity in RiceAtlas (Fig. 3) product (Laborte et al., 2017) were used to map the rice paddy area in the mapping results to planting/harvesting area to compare with statistical data since the area data they provide are all planting/harvesting area other than paddy area. The areas
 without single/double season information were defaulted to planting single-season rice.
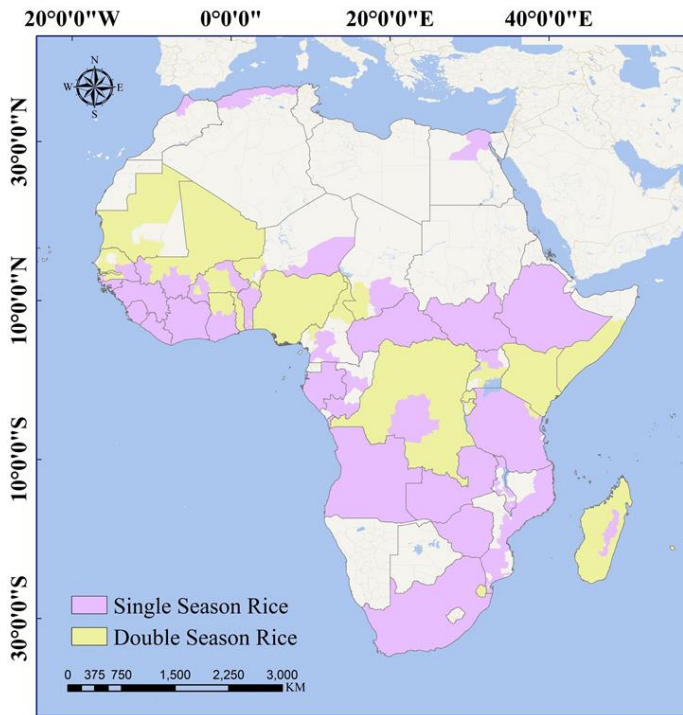
Figure 3. Administrative distribution map of rice intensity from ©RiceAtlas

To calculate the planting area, the paddy area is first derived from the mapping result. Then paddy area is allocated to the single season paddy area and the double season area according to the rice intensity map. Where

$$\text{Paddy Area} = \text{Single Season Paddy Area} + \text{Double Season Paddy Area} \qquad (1)$$

Then the planting area is calculated using:

$$\text{Planting Area} = \text{Single Season Paddy Area} + 2 * \text{Double Season Paddy Area} \qquad (2)$$

170
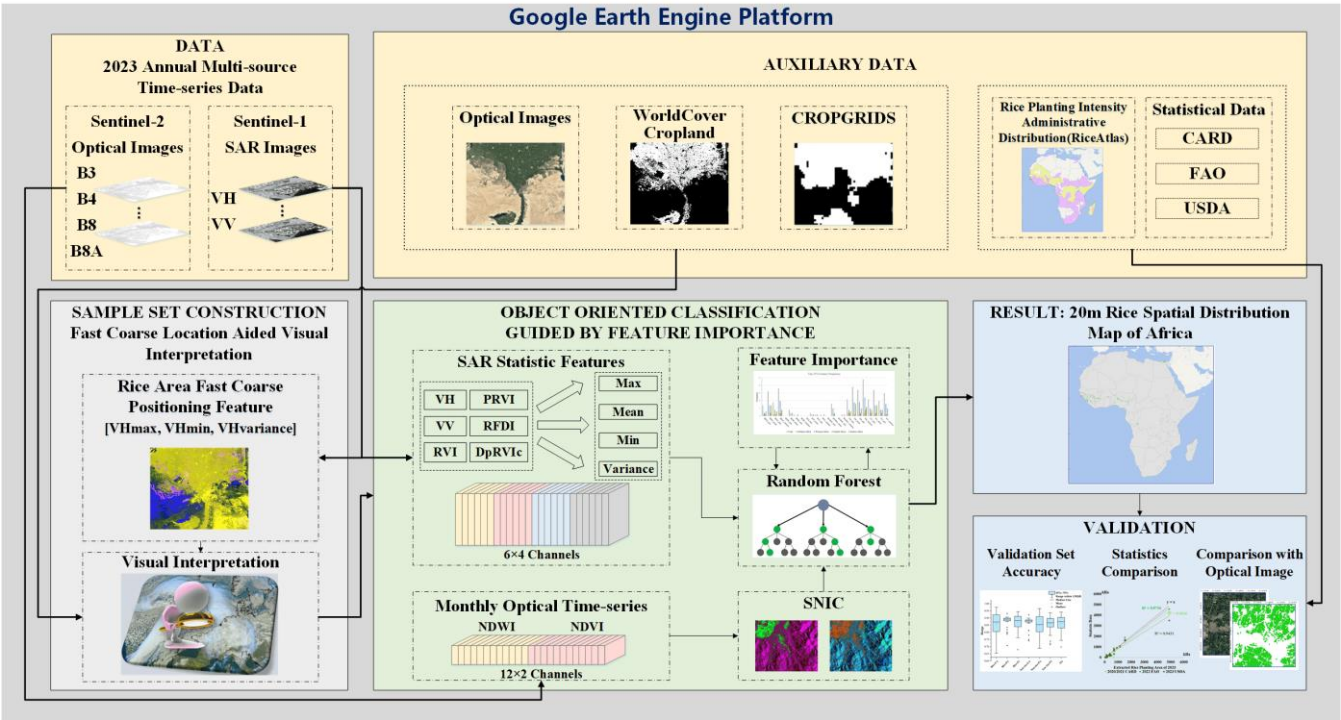
3 Method

Figure 4. Flowchart of the proposed rice mapping method (Optical images are from ©GoogleEarth)

The workflow for mapping the spatial distribution of rice in Africa at a 20-meter resolution is depicted in Fig. 4. The study adopts a multi-source time-series data approach combined with a supervised classifier to achieve large-scale, high-resolution mapping of rice distribution in Africa. The workflow is primarily divided into two main stages: sample set construction and object-based classification guided by feature importance.

During the sample set construction phase, visual interpretation is conducted referring to ESA WorldCover cropland data, CROPGRIDS rice grid map, and optical image, with statistical features from VH time series aiding in the fast coarse positioning of potential rice-growing regions.

During the classification phase, classification experiments were conducted in every country separately. Object-based segmentation is first performed on optical images to obtain super-pixel results, which helps mitigate the effects of speckle noise in SAR imagery, enhances classification accuracy, and better captures the complex spatial patterns of rice fields. The mean values of SAR data (VH, VV) and various radar vegetation indices derived from SAR data within these super-pixels are then used as input features. A random forest classifier is applied to train the model, which gives ranks of the importance of the input features. The most important features of different sub-regions of Africa are selected for a subsequent classification to produce the rice paddy distribution map. Finally, accuracy validation is conducted using statistical data and validation datasets.

3.1 Sample set construction: fast coarse positioning aided visual interpretation

3.1.1 Fast coarse positioning of rice planting area

Sun used the statistical features (max, min, variance) of VH time-series data for pseudo-color composite in rice mapping in Southeast Asia as input features for rice extraction (Sun et al., 2023), In the pseudo-color feature map (R: VH_{max}, G: VH_{min}, B: $VH_{variance}$), rice appears purple because VH_{min} is small, while VH_{max} and $VH_{variance}$ are larger mainly caused by the drop of VH backscattering during flooding period. This is true with both irrigated rice and rainfed rice in Southeast Asia in the literature. In the experiment, it was found that rice in Africa also exhibits similar behaviour, as shown in Fig. 5, for it is a common phenomenon for rainfed rice to experience temporary floods of different durations and depths caused by rainfall though not the same with the stable flooding period of irrigated rice (Yamamoto et al., 2012; Kwesiga et al., 2019; Panda and Barik, 2021; Mwakyusa et al., 2023). And it can be seen from Fig.5 that the rice planting region stands out distinctly in the feature map, making it easy to locate the general rice planting region. But it cannot be completely distinguished from ground objects like wetlands for their similarity in the feature map. Therefore, the feature map was only used for fast coarse positioning and preliminary screening of rice regions. Specific examples of selected rice fields are presented in Fig. 6.
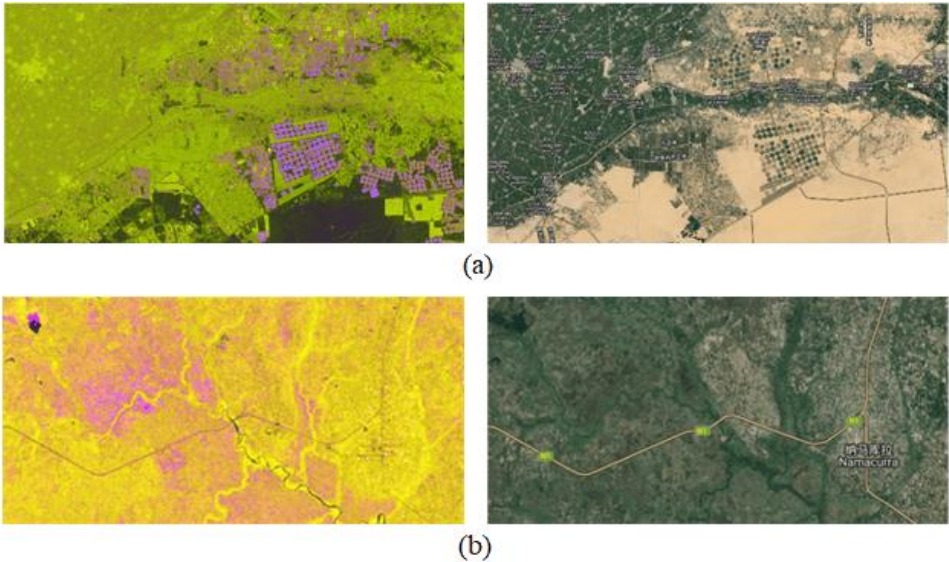
Figure 5. Pseudo-color composite image (R: VH_{max}, G: VH_{min}, B: $VH_{variance}$) used for fast coarse positioning, and corresponding optical image in Africa (From ©Google Earth) (a) irrigated region in Egypt(Mathieu, 2022) (b) rainfed lowland region in Mozambique(Kajisa and Vu, 2023). Examples of rice fields selected from these areas of Egypt and Mozambique are presented in Fig. 6.

3.1.2 Rice sample set construction

During the experiment, it was found that wetlands and other land cover types prone to misclassification with rice also appear as purple in the pseudo-color composite image described in Section 3.1.1. Therefore, multiple auxiliary datasets were used for visual interpretation to construct the rice sample set. Specifically, the process begins with positioning potential rice-planting areas using the fast coarse positioning feature. The intersection of the high-value rice grid map from CROPGRIDS and the cropland distribution map is then utilized to further narrow down these areas. Finally, rice plots are selected and confirmed as rice samples through visual interpretation of optical imagery. The cropland distribution maps used the union of the cropland classes from WorldCover for the years 2020 and 2021. Additionally, in some countries, existing studies or reports, as listed in Table 3, were consulted.

Table 3. Reference for rice sample set construction in some countries

Country	Reference
Benin	(Loko et al., 2022)
Burkina Faso	(Barro et al., 2021)
Egypt	(Mathieu, 2022)
South Sudan	(Fewsnet, 2018)

Generally, the rice plots have these features on optical images: (1) circular irrigation fields or fields with internal blocks or strips to retain water, especially near water, rivers, lakes, etc. (2) very uniform greenness and texture during the growing season. If the features are not clear enough, the time series curve of VH data would be examined for obvious fluctuations since the backscatter of VH polarized data of rice has a clear drop during the flooding period. Fig. 6 presents some examples of rice fields and the VH backscattering coefficient time series of the red-marked point. The field in Egypt is an example of the typical circular irrigated rice paddy during the growing season that can be located refer to the literature(Mathieu, 2022). The fields in Mali are in the irrigated region around Niono(Diuk-Wasser et al., 2007). The fields in Mozambique are an example of rainfed rice paddy during the growing season that can be located referring to the literature(Kajisa and Vu, 2023). The fields in Kenya are in the concentrated rice planting area in Mwea and can be located from (Menge et al., 2024), which are examples of rice fields with internal blocks or strips. The fields in Chad are part of the China-aided Bongor Rice Demonstration Base in Chad, which is an example of rice fields in the non-growing season (Liang et al., 2017). The fields in Madagascar are in Mahitsy where rice cultivation has a long history(Voahanyinirina and Elie, 2007). The corresponding pseudo-color composite feature map in Fig.6 also proves the effectiveness of the fast coarse positioning method.
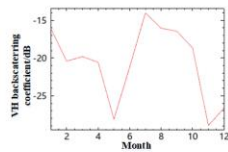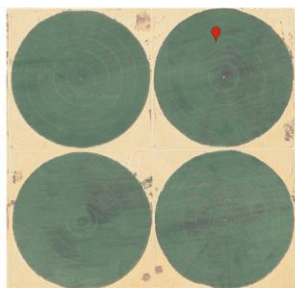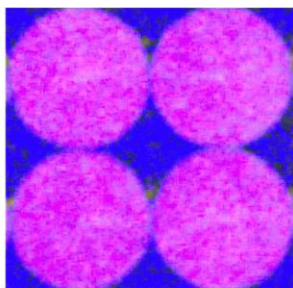
Giza, Egypt
30.22805N, 30.32874E
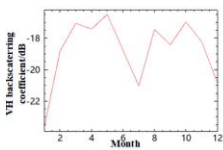
Niono, Mali
14.23381N, 5.97703W
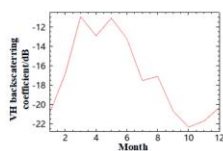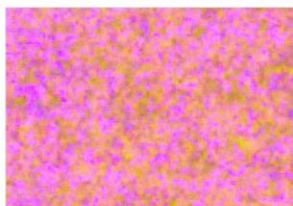
Namacurra, Zambézia, Mozambique
17.55638S, 37.06439E
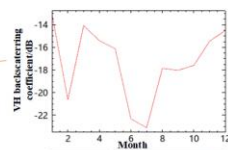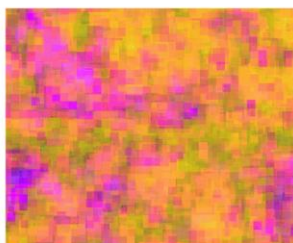
Mwea Rice farms, Kenya
0.67554S, 37.32479E
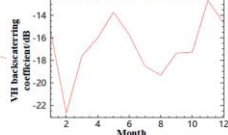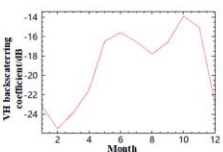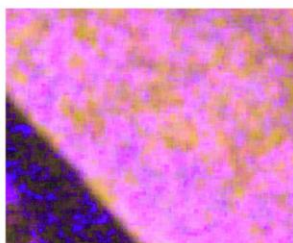
Kolobo, Bangor, Chad
9.93147N, 37.32479E
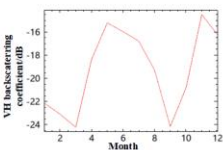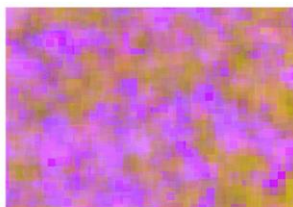
Mahitsy, Madagascar
18.74806S, 47.33491E

Figure 6. Examples of rice fields (a) Pseudo-color composite image (R: VHmax, G: VHmin, B: VHvariance) (b) Optical image(From ©Google Earth) (c) VH backscattering coefficient time series curve of the point marked in (b)

In the experiment, 50-300 rice plots were selected for each country, and 2000 rice points were randomly sampled from these plots as positive samples for the classifier input in each country's classification experiment.

3.1.3 Negative sample set

In the classification experiments conducted for each country, dozens of plots for each land cover type (non-rice cropland, built-up areas, water bodies, wetlands, forests, grasslands, etc.) were uniformly selected by visual interpretation based on optical imagery and the WorldCover product. For each land cover type, 300 sample points were randomly selected within these plots as negative samples for the classifier input.
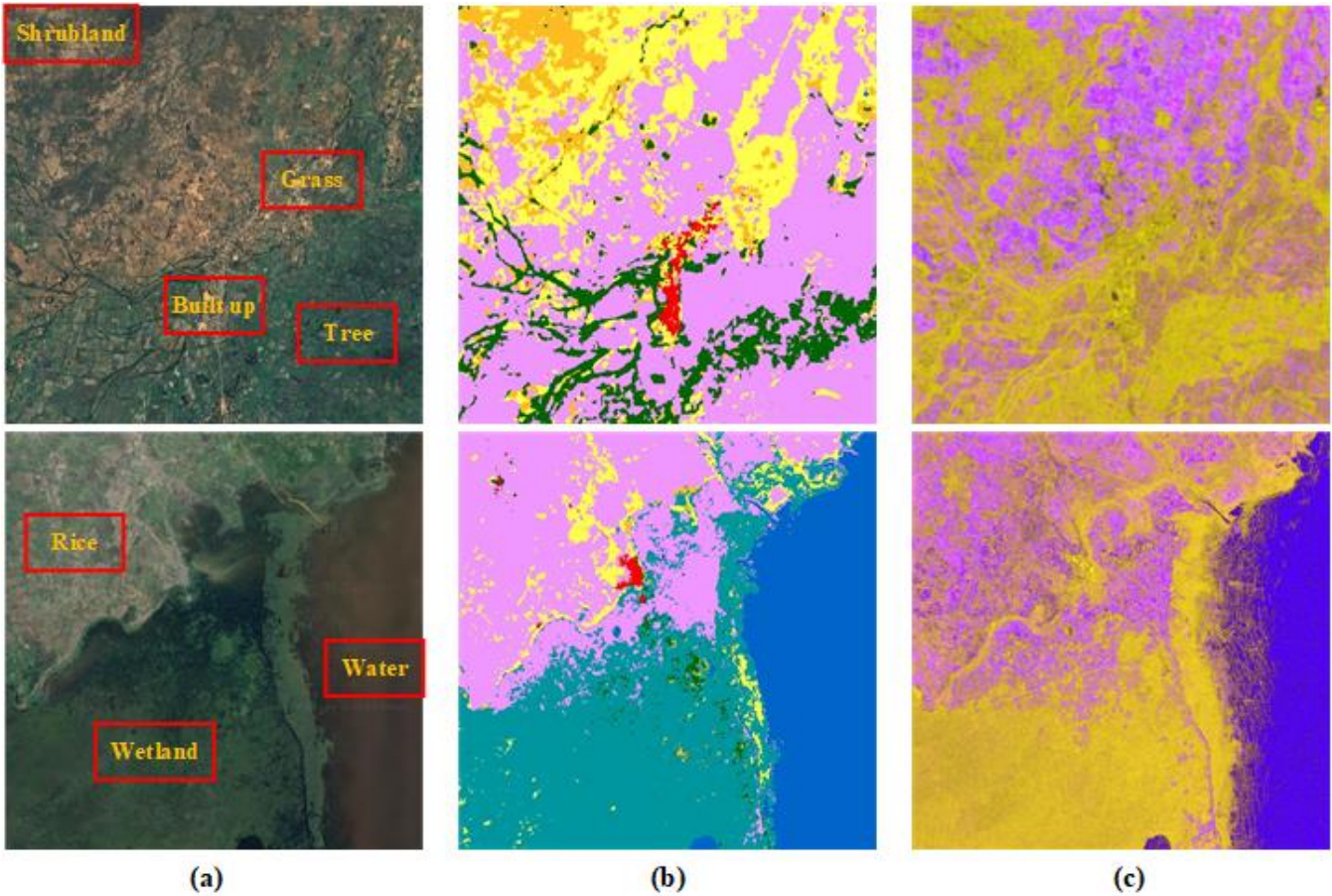
Figure 7. Example of positive and negative sample regions (a) Optical image (From ©Google Earth) (b) WorldCover2021 from ESA (c) the pseudo-color feature map (R: VHmax, G: VHmin, B: VHvariance)

3.1.4 Validation dataset

245 The validation dataset was constructed similarly to the training sample set. For each country, the validation dataset includes 1,000 rice sample points. Non-rice sample points were uniformly selected based on the number of land cover categories present in the WorldCover product for that country, with 100 sample points chosen for each category (with the cropland category containing only non-rice cropland samples).

3.2 Object-oriented supervised classification guided by feature importance

250 **3.2.1 SNIC object-oriented segmentation**

Monthly mean time series of NDWI and NDVI data from 2023 were used as inputs to perform object-based segmentation using the Simple Non-Iterative Clustering (SNIC) algorithm (Achanta and Susstrunk, 2017). This approach was adopted to reduce the fragmentation of rice paddy extraction results and enhance the clarity of rice paddy boundaries. The SNIC algorithm is a super-pixel segmentation method based on the principles of K-means clustering. It initializes seed points on a regular grid

255 as initial cluster centers and assigns each pixel to the nearest cluster based on its distance from the cluster center in both color and spatial dimensions. Since the SNIC algorithm is non-iterative, it requires less computation time and memory while ensuring connectivity, resulting in good segmentation performance. It is widely used in remote sensing applications (Tassi and Vizzari, 2020; Wang et al., 2024).

In the experiment, the SNIC algorithm was implemented on the GEE platform with the following parameter settings: seed

260 distance (size) = 10, segmentation compactness = 0.5, connectivity = 8, and neighbourhood size = 100. The effect of segmentation is demonstrated in Fig.8.

3.2.2 Feature importance guided supervised classification

To address the limitations of optical imagery caused by cloud cover in large-scale mapping, SAR features were utilized after object-based segmentation based on time-series NDVI and NDWI data. The mean values of the SAR features within the

265 segmented super-pixels were used as inputs for supervised classification to achieve more accurate large-scale, high-resolution rice mapping results. This part of the study employed the Random Forest algorithm available on the GEE platform. Supervised classification experiments were first conducted for each country, with all SAR data features used as inputs to determine feature importance rankings. The top-ranked features for each sub-region were then selected, and a second round of supervised classification was performed using these selected features to obtain the final mapping results.

270 The SAR features used in the experiment included VH, VV, and four commonly used radar vegetation indices: RVI (Radar Vegetation Index), PRVI (Polarimetric Radar Vegetation Index), RFDI (Radar Forest Degradation Index), and DpRVIc (Dual-pol radar vegetation index for GRD (Ground Range Detected) data). The statistical features (max, mean, min, variance) for these indices in 2023 were utilized, as defined in Table 4.

Table 4. Index definition

	Simplified Formula
RVI	$\frac{4*\sigma_{HV}}{\sigma_{VV}+\sigma_{HV}}$ (Charbonneau et al., 2005; Li and Wang, 2018)
PRVI	$\left(1-\frac{\sigma_{VV}}{\sigma_{VH}+\sigma_{VV}}\right)*\sigma_{VH}$ (Chang et al., 2018; Sun et al., 2024)
RFDI	$\frac{\sigma_{HH}-\sigma_{HV}}{\sigma_{HH}+\sigma_{HV}}$ (Chhabra et al., 2022)
DpRVIc	$q*\frac{q+3}{(q+1)^2}, q=\frac{\sigma_{HH}}{\sigma_{HV}}$ (Bhogapurapu et al., 2022)

3.3 Accuracy on validation set

The validation section first performs on the validation set, calculating the user accuracy (UA), producer accuracy (PA), F1-score, and overall classification accuracy (OA) for rice and non-rice categories:

$$UA = \frac{TP}{TP+FP} \tag{3}$$

$$PA = \frac{TP}{TP+FN} \tag{4}$$

$$F1 = 2 \times \frac{UA \times PA}{UA+PA} \tag{5}$$

$$OA = \frac{TN+TP}{TN+TP+FN+FP} \tag{6}$$

Where TP is true positive, FP is false positive, TN is true negative, and FN is false negative.

4 Results

In this section, the results and accuracy will be presented from five aspects: feature screening results, mapping and analysis of rice spatial distribution, comparison of rice area statistics results, validation set accuracy, and comparison of optical images.

4.1 Feature importance

Due to the few coverage of SAR images in Angola and Sudan, these two countries only use optical images as classification input features. In the experiments of the remaining 32 countries, a total of 24 statistical features (max, mean, min, and variance) of VH, VV, RVI, PRVI, RFDI, and DpRVIc were input into random forest training to obtain feature importance ranking results. The frequency of each feature in the top 25% of feature importance ranking for each country was calculated according to the

UN (United Nations) divided African sub-region, as shown in Fig. 8 (a). The features marked red are the selected features used in classification experiments for final mapping.

Total		Northern		Western		Central		Eastern	
Feature/Frequency		Feature/Frequency		Feature/Frequency		Feature/Frequency		Feature/Frequency	
VH_variance	23	PRVI_variance	2	VH_variance	24	VH_variance	4	VH_mean	8
VH_mean	18	VH_max	2	VH_mean	19	PRVI_mean	2	PRVI_mean	7
PRVI_variance	17	VH_variance	2	PRVI_variance	18	PRVI_variance	2	VV_mean	7
VH_min	17	PRVI_max	1	VH_min	17	VH_max	2	VH_variance	6
PRVI_mean	16	PRVI_min	1	VV_mean	17	VH_min	2	VH_min	5
VV_mean	16	VH_mean	1	PRVI_mean	16	VV_max	2	VV_variance	5
VV_variance	15	VH_min	1	VV_variance	15	VV_mean	2	PRVI_variance	4
VV_max	11	VV_mean	1	VH_max	11	VV_min	2	VV_max	4
VH_max	10	VV_variance	1	VV_max	11	PRVI_max	1	VV_min	4
VV_min	10	PRVI_mean	0	VV_min	10	PRVI_min	1	PRVI_max	3
PRVI_min	9	RFDI_max	0	PRVI_min	9	DpRVIc_mean	1	PRVI_min	3
DpRVIc_mean	8	RFDI_mean	0	DpRVIc_mean	8	DpRVIc_variance	1	VH_max	3
PRVI_max	6	RFDI_min	0	PRVI_max	7	VH_mean	1	RFDI_mean	2
RFDI_mean	4	RFDI_variance	0	RFDI_mean	4	VV_variance	1	DpRVIc_mean	2
RVI_mean	2	RVI_max	0	RVI_mean	2	RFDI_max	0	RFDI_min	1
RFDI_min	1	RVI_mean	0	RFDI_min	1	RFDI_mean	0	RVI_mean	1
RVI_min	1	RVI_min	0	RVI_min	1	RFDI_min	0	RVI_variance	1
RVI_variance	1	RVI_variance	0	RVI_variance	1	RFDI_variance	0	RFDI_max	0
DpRVIc_variance	1	DpRVIc_max	0	DpRVIc_variance	1	RVI_max	0	RFDI_variance	0
RFDI_max	0	DpRVIc_mean	0	RFDI_max	0	RVI_mean	0	RVI_max	0
RFDI_variance	0	DpRVIc_min	0	RFDI_variance	0	RVI_min	0	RVI_min	0
RVI_max	0	DpRVIc_variance	0	RVI_max	0	RVI_variance	0	DpRVIc_max	0
DpRVIc_max	0	VV_max	0	DpRVIc_max	0	DpRVIc_max	0	DpRVIc_min	0
DpRVIc_min	0	VV_min	0	DpRVIc_min	0	DpRVIc_min	0	DpRVIc_variance	0

(a)

(b)
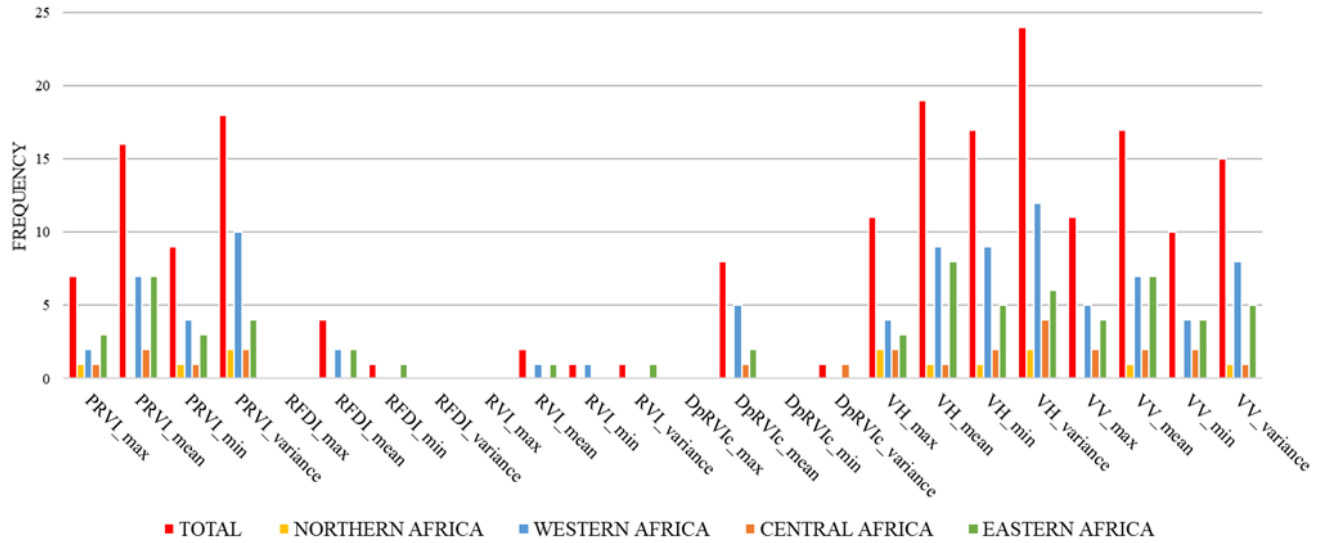
Figure 8. Feature importance (a) Regional statistics on the frequency of features appearing in the top 25% of importance rankings

295   **(descending order) (b) Regional statistics on the frequency of features appearing in the top 25% of importance rankings (sort by feature)**

In Fig.8 (a), the features highlighted in red represent those with the highest frequency within the top 25% of importance rankings for each region (including features with tied frequencies). It can be observed that the top 25% features vary significantly across sub-regions, with the only common feature being VH_variance. Therefore, in the Random Forest

300   supervised classification, each sub-region used the features ranked in the top 25% in frequency for that specific sub-region.

Fig. 9 illustrates an example of selected features, focusing on an area southwest of Lake Alaotra in Madagascar. The classification features used in the supervised classification for this region include six features specific to East Africa: VH_mean, PRVI_mean, VV_mean, VH_variance, VH_min, and VV_variance. These features were combined into two groups for pseudo-color composites, where clear distinctions between rice fields and other land cover types, including wetlands and grasslands

305   that are prone to misclassification, can be observed. Zoomed-in images are provided in the third column. The contrast of rice and non-rice fields, the field ridges, and the consistency with optical images can be observed clearly. This demonstrates that the selected features effectively differentiate rice from other land cover types, enabling accurate spatial mapping of rice distribution. Additionally, the mean values calculated from object-based segmentation of optical imagery improved the representation of SAR image noise and fragmented plots while preserving clear boundaries.
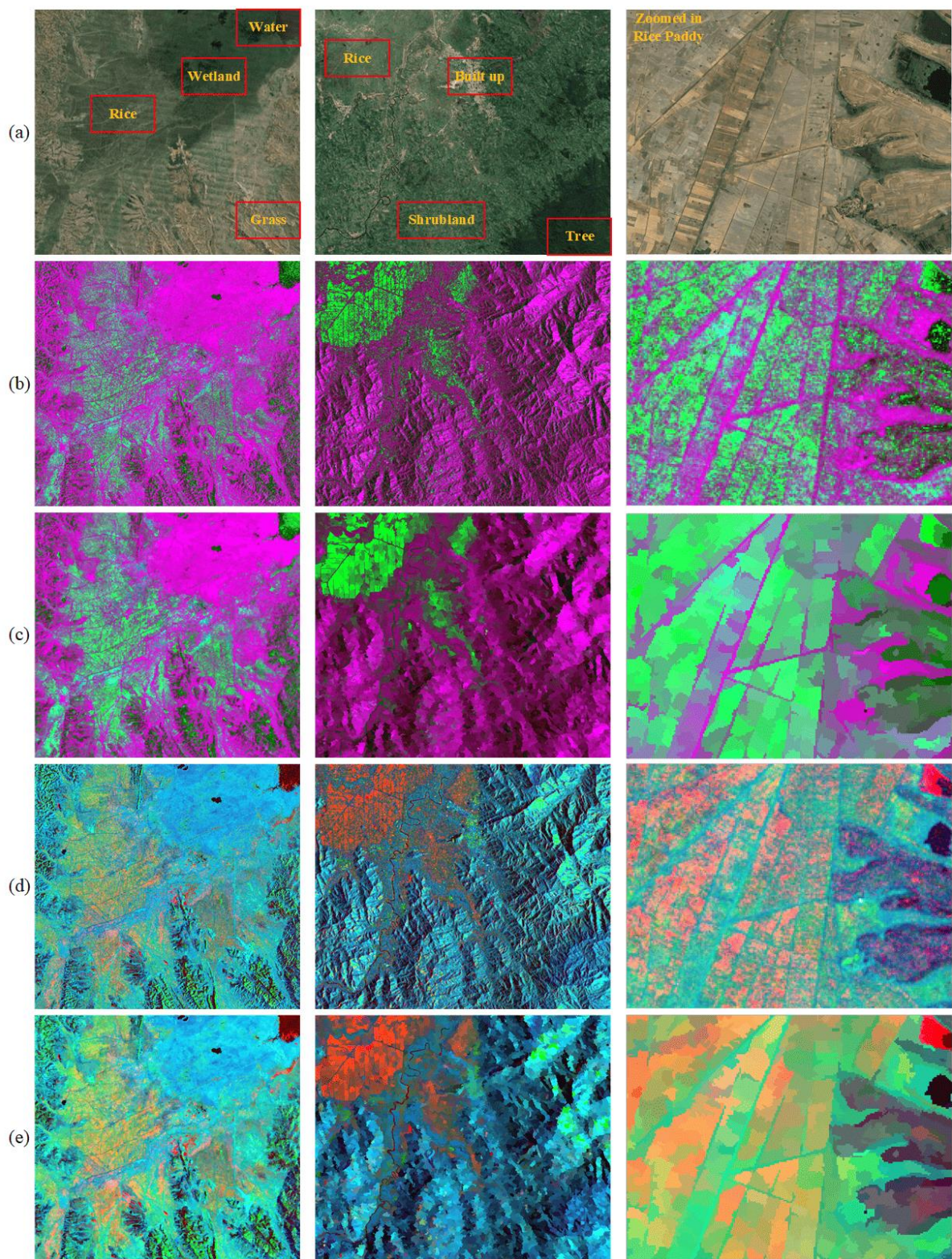
Figure 9. Example of pseudo-color composites using selected time-series SAR features: (a) optical image(From ©Google Earth) (b) pseudo-color composite 1 (R: VH_min, G: VH_variance, B: VH_mean) (c) mean values of pseudo-color composite 1 overlaid on the object-based segmentation result from NDVI time series (d) pseudo-color composite 2 (R: VV_variance, G: VV_mean, B: PRVI_mean); (e) mean values of pseudo-color composite 2 overlaid on the object-based segmentation result from NDVI time series.

4.2 Results of rice spatial distribution map

Fig. 10 shows the final 20-meter resolution spatial distribution map of rice across Africa. The green areas represent rice. The map on the right displays the gridded result at a 0.5-degree resolution, with the value in the lower left corner of each grid indicating the rice area, measured in 100 hectares per grid.
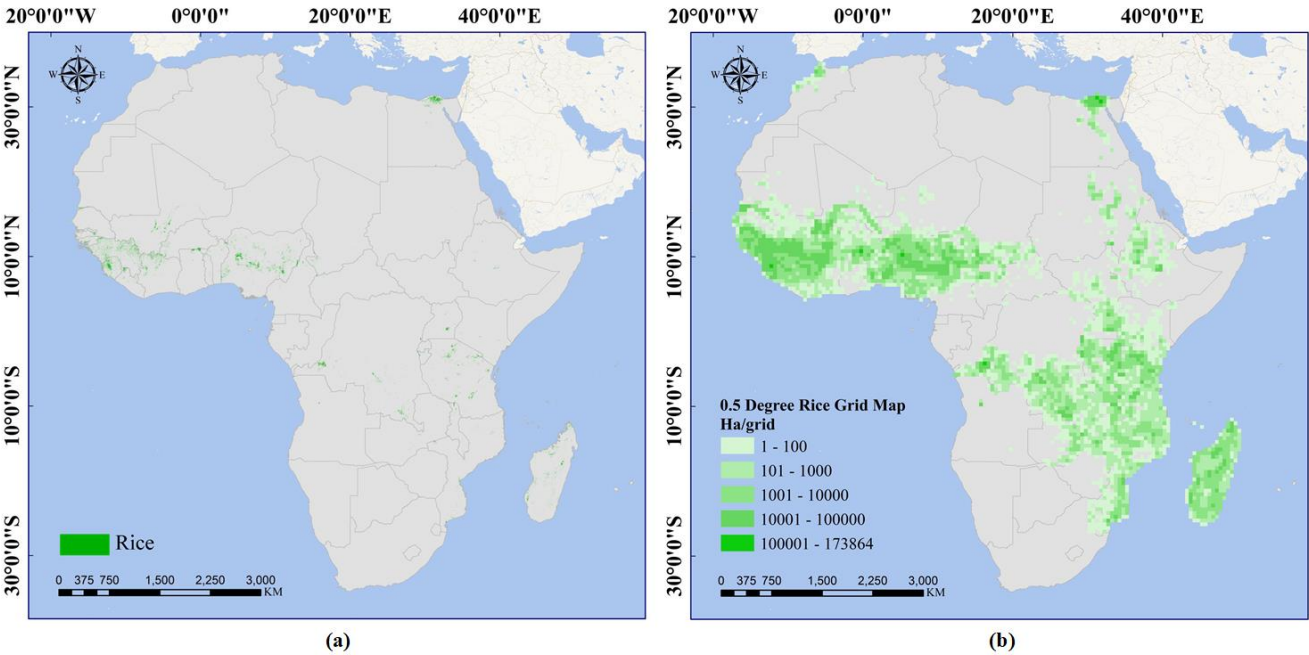
Figure 10. Rice mapping result in Africa (a) 20-meter spatial distribution map (b) corresponding 0.5° grid map

Table 5. Country-level statistics of rice paddy area in Africa based on the 20m spatial distribution map for 2023.

No.	Country	Paddy Area/Ha	No.	Country	Paddy Area/Ha
1	Angola	30375	18	Madagascar	865405
2	Benin	149095	19	Malawi	120866
3	Burkina Faso	205356	20	Mali	502970
4	Burundi	53626	21	Mauritania	63672
5	Cameroon	210191	22	Morocco	40454
6	Central African Republic	70545	23	Mozambique	415471
7	Chad	283113	24	Niger	45410

8	Côte d'Ivoire	727320	25	Nigeria	2446413
9	Democratic Republic of the Congo	841988	26	Rwanda	30984
10	Egypt	689114	27	Senegal	202077
11	Ethiopia	155157	28	Sierra Leone	694314
12	Gambia	103316	29	South Sudan	48605
13	Ghana	355311	30	Sudan	52553
14	Guinea	1580359	31	Togo	97076
15	Guinea-Bissau	178277	32	Uganda	199103
16	Kenya	29610	33	United Republic of Tanzania	1088377
17	Liberia	135214	34	Zambia	83916

Table 5 presents the country-level statistics of rice paddy area in Africa based on the 20m spatial distribution map for 2023. The total rice paddy area across Africa in 2023 is approximately 12,795,631 hectares. Among the countries, three have rice areas exceeding 1 million hectares: Nigeria, Guinea, and Tanzania. Six countries fall within the range of 500,000 to 1 million hectares: Madagascar, the Democratic Republic of Congo (DRC), Côte d'Ivoire, Sierra Leone, Egypt, and Mali. Thirteen countries have rice areas between 100,000 and 500,000 hectares: Mozambique, Ghana, Chad, Cameroon, Burkina Faso, Senegal, Uganda, Guinea-Bissau, Ethiopia, Benin, Liberia, Malawi, and Gambia. Lastly, twelve countries have rice areas between 50,000 and 100,000 hectares: Togo, Zambia, Central African Republic, Mauritania, Burundi, Sudan, South Sudan, Niger, Morocco, Kenya, Rwanda, and Angola. The proportion of rice area by country is illustrated in Fig. 11(a).
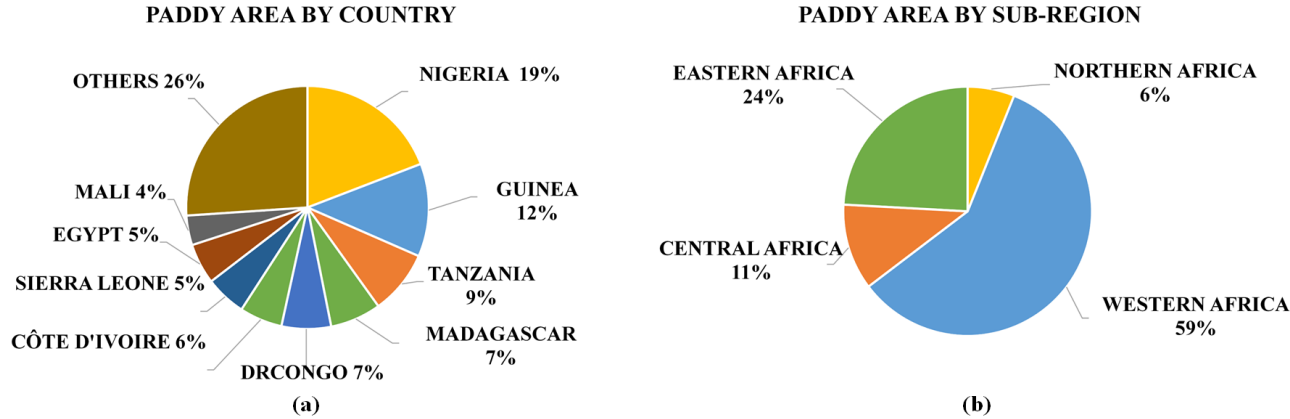
Figure 11. The proportions of rice paddy area in Africa (a) by country (others: aggregate of countries with areas less than 500,000 hectares). (b) by sub-region

Fig. 11(b) shows the distribution of rice area by sub-region in Africa. It can be seen that rice planting is primarily concentrated in Western Africa, followed by Eastern Africa and Central Africa, with the least in Northern Africa. The specific distribution of major production areas is detailed in Table 6.

Table 6. Distribution of Major Rice-Producing Regions in Africa

Northern Africa	
Egypt	Predominantly located in the Nile Delta and the Faiyum Oasis.
Western Africa	
Nigeria	Concentrated along the western side of the Kainji Reservoir, as well as along the Niger, Benue, Sokoto, and other rivers and their tributaries.
Guinea	Mainly distributed in the coastal plains of the Boffa region in the west, the plains of the Koundara region in the northwest, and along the Niger and Sankarani rivers and their tributaries in the east.
Mali	Primarily located along the Niger River and its tributaries in the central and eastern regions.
Sierra Leone	Concentrated in the western plains.
Côte d'Ivoire	Mainly found along the Bandama River in the northwest, the Bafing region in the west, and the northern areas.
Central Africa	
Democratic Republic of the Congo	Predominantly located near Kinshasa and around Lake Mukamba.
Eastern Africa	
Tanzania	Concentrated in the Mapogoro and Itambaleo regions, the southern areas of Lake Victoria, southern Morogoro, and the Kilimanjaro region.
Madagascar	Mainly distributed in the western regions of Lake Alaotra, southwestern areas, and the Ankililoaka region.

4.3 Comparison of rice area and statistical data

Table 7 presents the statistical data of rice planting areas for 34 African countries with more than 5,000 hectares of rice area, listed in alphabetical order. The first column shows the rice planting/harvest area reported by the Coalition for African Rice Development (CARD) for its member countries in 2020/2021. The second column provides the 2022 rice harvest area data from FAO. The third column shows the 2023 rice planting/harvest area reported by USDA. The fourth column presents the 2023 rice planting area derived from this study using the rice intensity data of RiceAtlas. All area units are in hectares.

Table 7. Rice Area Statistics for African Countries

No.	Country	2020/2021 CARD /Ha	2022 FAO Harvest/ Ha	2023 USDA/Ha	Planting Area/Ha
1	Angola	8572	8572	8000	30375
2	Benin	134840	134840	135000	215851
3	Burkina Faso	221052	198473	220000	273063
4	Burundi	50478	54441	0	102335
5	Cameroon	296209	156739	285000	403379
6	Central African Republic	8596	36981	/	70545
7	Chad	184086	177108	190000	501287
8	Côte d'Ivoire	581766	688201	730000	727320
9	Democratic Republic of the Congo	1442356	1888472	1660000	1523243
10	Egypt	/	646316	630000	689114
11	Ethiopia	60000	60000	60000	155157
12	Gambia	60097	46418	65000	206632
13	Ghana	414027	305000	325000	709060
14	Guinea	1650217	1627939	1650000	1580359
15	Guinea-Bissau	126654	130291	120000	178277
16	Kenya	82330	29615	30000	59220
17	Liberia	240000	257000	240000	135214
18	Madagascar	1600000	1598207	1600000	1537131
19	Malawi	76962	75787	/	120866
20	Mali	874031	888116	920000	914169
21	Mauritania	/	71000	75000	126846
22	Morocco	/	6320	8000	40454
23	Mozambique	282000	290000	290000	415471
24	Niger	12566	32414	30000	85573
25	Nigeria	4320100	4580000	3500000	4889668
26	Rwanda	31676	32253	/	61969
27	Senegal	370750	372413	370000	384397
28	Sierra Leone	944450	688549	825000	694314
29	South Sudan	/	30718	/	48605
30	Sudan	8513	10753	/	52553

31	Togo	98133	99958	94000	194153
32	Uganda	101325	260000	200000	368356
33	United Republic of Tanzania	955729	998000	1100000	1160821
34	Zambia	59601	39581	/	83916

(a) (b) (c)
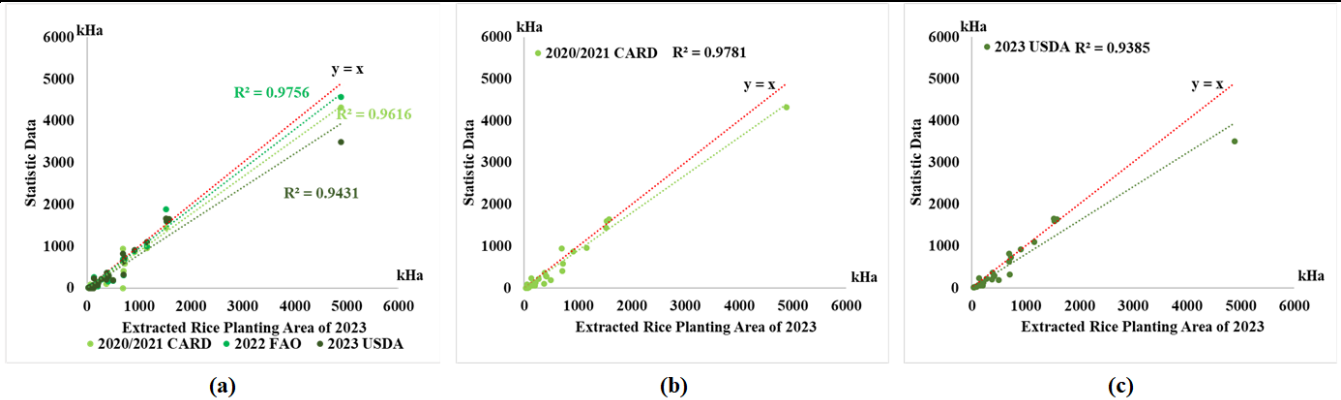
Figure 12. The linear fitting results between the 2023 rice planting area derived from this study and the existing statistical data, with mapping results as the x-axis and existing statistical data as the y-axis. The red dashed line represents the y = x line. (a) fitting results for all 34 countries, (b) fitting results for 30 countries after excluding those with missing data from the CARD dataset (c) fitting results for 27 countries after excluding those with missing data from the USDA dataset.

350   The comparison between the calculated rice planting areas from the mapping result and the rice intensity distribution data, alongside existing statistical data, reveals a strong linear relationship, as shown in Fig. 13. For all 34 countries, the R² value for fitting with CARD data (2020/2021) is 0.9616, with FAO data (2022) is 0.9756, and with USDA data (2023) is 0.9431. After excluding countries with missing data, the R² for fitting with CARD data (30 countries) improves to 0.9781, while for USDA data (27 countries) it is 0.9385, demonstrating strong consistency.

355   The figures and tables indicate that in countries with relatively low rice cultivation, the mapped areas generally exceed existing statistical data, shown as points below the y = x line in the fitting plot. In contrast, for countries with larger rice cultivation areas—such as the Democratic Republic of the Congo, Egypt, Guinea, Madagascar, Mali, and Tanzania—the mapped areas closely match existing statistics, with data points near the y = x line. While in Nigeria, the mapped rice cultivation area is significantly higher than existing statistics, represented by points far below the y = x line.

360   These discrepancies may be attributed to several factors. In developing countries in Africa, data collection and reporting systems are often incomplete and inconsistent, leading to major gaps in the accuracy of reported rice cultivation areas. The issue is further compounded by the dominance of smallholder farming systems, where individual farm sizes are smaller and scattered, making them even harder to track and report on accurately. This often results in underreporting or outdated figures in official statistics. Additionally, rice cultivation in these regions has undergone rapid changes in recent years, with some

365   areas seeing significant increases in planting that aren't being fully captured by traditional reporting methods. Although multiple auxiliary datasets were integrated when constructing the rice sample set for this study, the process still heavily relied

on expert knowledge. This is particularly challenging in countries with limited rice cultivation, where rice fields are more difficult to identify, leading to sample errors that directly affect mapping accuracy. Moreover, the rice intensity distribution information used to estimate planting areas was published in 2017 and may not fully capture the present situation in 2023, contributing to discrepancies between the mapped data and reported cultivation areas.

4.4 Classification accuracy on the validation set

The validation results for rice and non-rice classifications across 34 African countries provide a comprehensive insight into the model's performance. Fig. 13 displays key metrics, including user accuracy (UA), producer accuracy (PA), F1 scores, and overall accuracy (OA). Analyzing these metrics offers an understanding of the spatial variations and classification challenges encountered across different regions.

Rice Classification Performance:

User Accuracy (UA): The UA for rice classification ranges from 65.26% in South Sudan to 97.51% in Rwanda. The lower values in countries like South Sudan and Niger highlight challenges in correctly identifying rice fields, possibly due to fragmented land use or small cultivation areas.

Producer Accuracy (PA): The PA for rice classification spans from 70.78% in South Sudan to 93.17% in Guinea. Higher PA values indicate the model's ability to correctly classify most rice areas, while lower values in regions like South Sudan suggest a tendency for rice areas to be misclassified as non-rice.

F1 Score: The F1 scores, combining precision and recall, vary from 67.91% in South Sudan to 94.54% in Guinea. While most countries maintain F1 scores above 80%, lower scores in regions like Angola and Niger highlight difficulties in balancing precision and recall.

Non-Rice Classification Performance:

User Accuracy (UA): The UA for non-rice ranges from 74.09% in South Sudan to 92.18% in Guinea, with most countries over 85%. High UA values across most countries indicate effective identification of non-rice areas.

Producer Accuracy (PA): The PA ranges from 68.92% in South Sudan to 96.55% in Rwanda. Most countries exceed 80%, underscoring consistent performance, though lower values in South Sudan indicate difficulties in distinguishing non-rice areas.

F1 Score: The F1 scores for non-rice range from 71.41% in South Sudan to 93.74% in Guinea. Countries with lower scores, such as Niger and Sudan, highlight specific regional challenges in sample set construction with very limited rice cultivation.

Overall Accuracy (OA):

The overall accuracy (OA) ranges from 69.76% in South Sudan to 94.17% in Guinea, with a mean of around 86.30%. Of all countries in the study site, one country has OA under 70% (South Sudan), 4 countries between 70% and 80% (Niger, Zambia, Angola, and Sudan). All these countries have small area of rice, posing extra challenges to sample set construction. When the rice paddy area of a country is too small compared to the total land area, the rice plots we can locate are very limited since wetlands are similar to rice paddies in the feature map, which has far larger area causing rice paddies to look like scattered noise, hence the relatively lower OA in these countries. But countries with extensive rice cultivation, such as Ghana and

Senegal, show OAs above 90%, reflecting the model's robustness in regions with more homogeneous and concentrated rice production.

Key Insights and Implications:

Regional Variations: The variations in accuracy metrics indicate that regional agricultural practices, land use complexity, and data quality play significant roles in model performance. Regions with small, fragmented rice fields or mixed cropping systems, such as South Sudan, Niger, and Angola, present classification challenges that lead to lower accuracy scores.

Outliers and Challenges: The box plot (Fig.14 (b)) analysis reveals stable and consistent performance across most countries, with median values clustering between 85% and 90%. However, outliers such as South Sudan, Angola, and Niger show lower accuracy scores, mainly caused by lack of sufficient rice samples, suggesting that additional refinement is needed for these regions.

Model Reliability: The overall consistency in accuracy metrics across most countries highlights the robustness of the rice mapping methodology. Future improvements could focus on addressing the specific challenges faced in regions with complex agricultural landscapes or limited data availability.

The findings underscore the importance of tailored approaches when applying classification models across diverse African environments. Addressing regional discrepancies will be crucial in enhancing data accuracy and supporting better agricultural policy development across Africa.
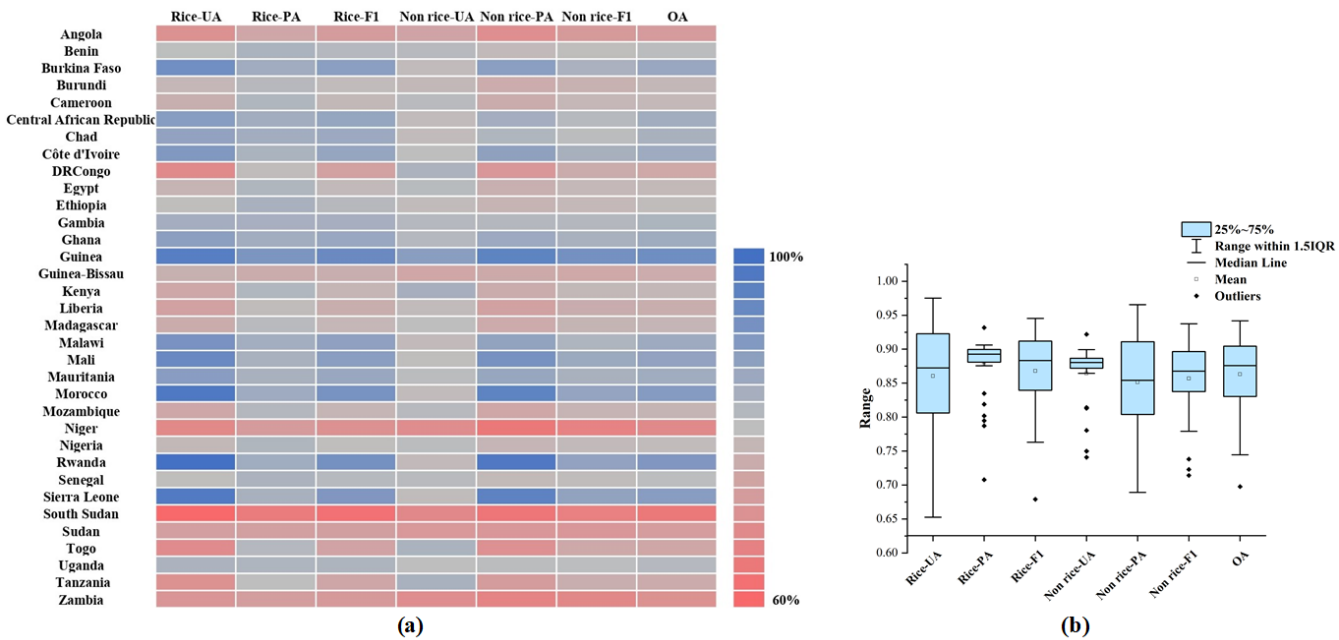
Figure 13. Performance on the validation set (a) heat map of validation accuracy across 34 African countries (b) corresponding box plot

4.5 Comparison of rice mapping results with optical imagery

420 Fig. 14 illustrates the comparison between the rice mapping results and corresponding optical images for selected regions in nine major rice-producing countries in Africa (with rice field areas exceeding 500,000 hectares). The examples include both concentrated plantation zones and dispersed smallholder farming areas. The results show a strong alignment between the mapped outputs and the optical images. Additionally, due to the incorporation of the object-based segmentation step, the mapping results exhibit clear boundaries, minimal scattered noise, and fewer misclassifications.
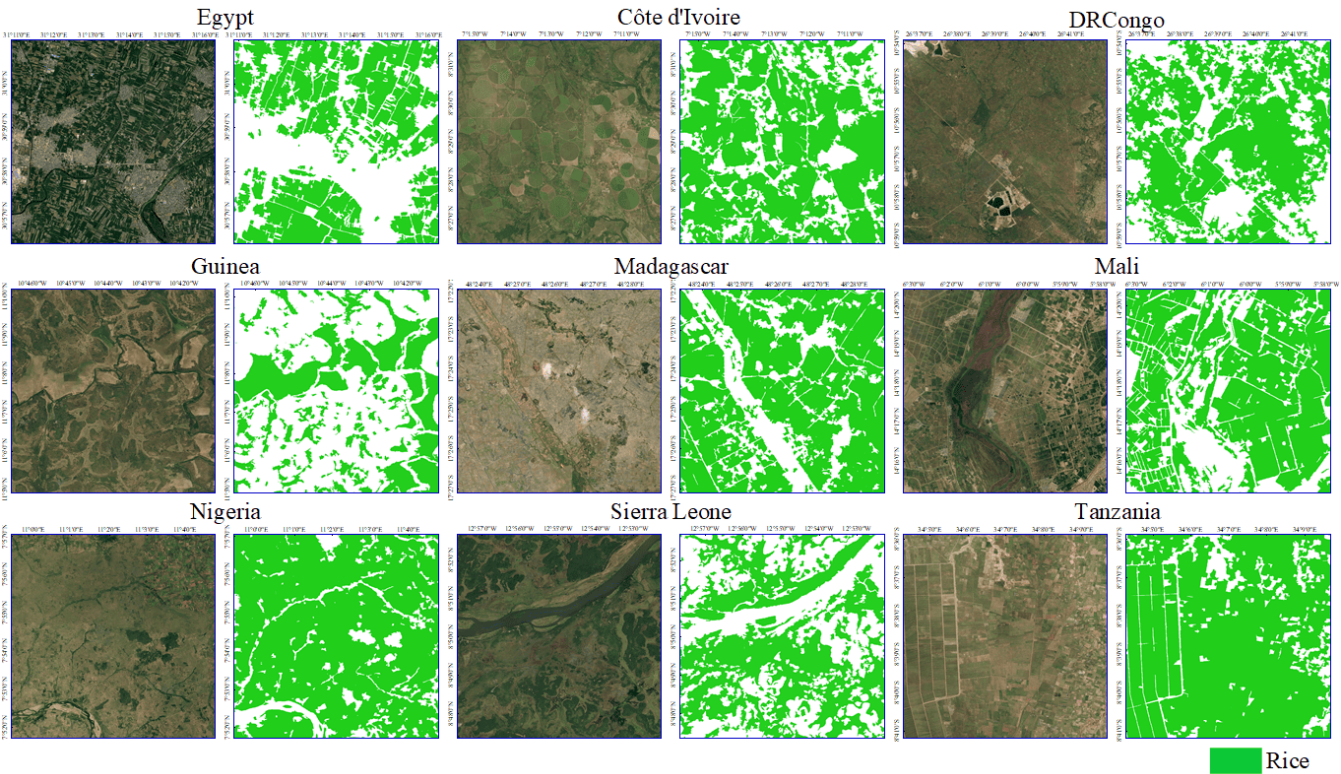
425

Figure 14. Examples of rice mapping results and corresponding optical imagery for major rice-producing countries in Africa. For each country, the first row shows the optical imagery (from ©Google Earth), while the second row presents the rice mapping results, with green areas representing rice fields.

5 Discussion

5.1 Strengths and limitations

430 To produce large-scale, high-resolution rice distribution maps across Africa, this study proposed a method effectively combining Sentinel-1 SAR and Sentinel-2 optical imagery, addressing key challenges in sample collection and classification. By leveraging time-series statistical features from Sentinel-1 VH data for initial fast coarse positioning of potential rice-planting areas and complementing this with visual interpretation using auxiliary datasets, the study efficiently generates

435 reliable samples. During the classification phase, the approach integrates object-based segmentation results from Sentinel-2 optical time-series data with feature importance guided Random Forest classification results from Sentinel-1 SAR time-series data. This combination enhances the precision of rice paddy boundaries and reduces noise in heterogeneous landscapes, showing a significant improvement over pixel-based methods. Additionally, the proposed method requires no phenology information, allowing for a more adaptable mapping process across diverse rice-growing regions like Africa, avoiding the

440 inaccuracies that arise from seasonal variability and diverse planting practices, which are common challenges in phenology-based methods. Collectively, these strengths underscore the method's robustness, efficiency, and scalability, positioning it as a reliable tool for high-resolution agricultural monitoring across Africa.

Despite these strengths, the study acknowledges limitations related to the SNIC algorithm, particularly in the calibration of key parameters—seed distance and neighbourhood size, which affects the size and definition of segmented objects. In this

445 study, it was primarily achieved through a process of trial and visual inspection. While this method provided a practical solution within the context of this research, the robustness of the method needs to be further strengthened. Future research should focus on developing more systematic approaches to parameter optimization. This could involve the use of automated tuning algorithms or machine learning techniques that adjust parameters dynamically based on the characteristics of the input data, thereby improving the accuracy, consistency, and scalability of the segmentation process.

450 Another potential problem is when comparing with statistical data, the administrative distribution data of rice planting intensity in RiceAtlas product is utilized to calculate the planting area from the paddy area of the mapping result. This dataset of the year 2017 could lead to gaps among the calculated planting area, actual planting area, and statistical data since rice cultivation has expanded rapidly in recent years as mentioned in section 4.3. However, there is no up-to-date dataset of rice intensity in Africa. And other datasets including rice intensity in Africa like GCI (Global Cropping Intensity) from year 2001 to 2019 (Liu

455 et al., 2021), and GCI30(Zhang et al., 2021) from year 2016 to 2018, are pixel-level datasets, which are assumed to change more than administrative-level data over time. Therefore, RiceAtlas is chosen as the rice intensity source to balance consistency and data availability and only used to fit with statistics to demonstrate the reliability of our result. Nevertheless, more up-to-data intensity data can provide more insight into the rice planting status in Africa.

Moreover, the sample set in this study was constructed through visual interpretation, assisted by the fast coarse positioning

460 feature. As discussed in the overall accuracy part of Section 4.4, when conducting sample set construction in countries with very small areas of rice (such as South Sudan, Niger, Zambia, Angola, and Sudan), the difficulty to locate rice plots is still huge since ground objects like wetlands are similar to but much more than rice paddies in the feature map, resulting lower OA in these countries. To enhance the mapping accuracy in such countries, the current mapping results could serve as a reference to develop an expanded sample set for a new round of training and classification in future work. Given the relatively small

465 spatial extent of these regions compared to the entire African continent, the spatial heterogeneity is significantly reduced. This allows for a more detailed analysis of rice phenology, which could substantially improve mapping performance. To improve the effectiveness of the proposed method of mapping rice at a large scale, weakly supervised learning algorithms could be

employed to automatically augment the training sample set and improve classification accuracy in future studies. The sample expansion process could still be guided by feature importance to ensure the reliability and robustness of the generated samples.

470 **5.2 Enlightenment and implications**

The experiment result highlights regional variations in the importance of specific features for rice mapping across Africa. Despite these variations, temporal statistical features from SAR data—particularly VH, VV, and PRVI—consistently demonstrated their utility in capturing the temporal dynamics of rice cultivation. By further exploring and experimenting with these temporal SAR features, future studies could refine rice detection models to be more sensitive to regional differences and

475 temporal changes in Africa. This could involve integrating these features with additional data sources, such as optical imagery or other environmental variables, to create more robust and comprehensive mapping models.

The rice distribution map generated in this study has significant implications for agricultural monitoring and food security across Africa. By providing an accurate baseline for rice distribution, this study supports government and research initiatives focused on food resource management, land use planning, and climate impact assessments. Unlike current rice mapping studies

480 in Africa, which have been constrained by limited spatial resolution and are primarily represented as gridded data, this approach offers a reliable, scalable framework that aligns with Africa's need for consistent agricultural data.

5.3 Progress and gaps in the National Rice Development Strategy (NRDS) of CARD countries towards 2030 targets

Comparing existing rice planting/harvesting statistics from African countries with the rice planting area results obtained in this study reveals that although rice cultivation in most African countries has fluctuated, there is still a slow upward trend. This

485 aligns with the policy direction of promoting rice cultivation in these countries, though there remains a significant gap to achieve the 2030 Rice Research and Innovation Strategy for Africa target. Table 8 and Fig. 15 present the targets of rice planting area and the completed percentage of countries in CARD. Among the countries assessed, 15 have achieved over 80% of the 2030 target, 5 have achieved 60–80%, 7 have achieved 40–60%, and 3 have achieved less than 40%. Of the 9 countries with completion rates below 60%, Tanzania, Senegal, Sierra Leone, and Burkina Faso currently have substantial rice

490 cultivation areas (greater than 200,000 hectares) but have set high targets. Ethiopia, Liberia, Sudan, Niger, and Kenya have smaller targets but still lag in their current rice cultivation. Countries should develop and adjust their rice cultivation strategies accordingly to achieve the "Transformation of Rice-based Agri-food Systems for Food and Nutrition Security in Africa" and enhance local food self-sufficiency, ultimately contributing to the SDGs (Sustainable Development Goals) of zero hunger.

Table 8. Current rice cultivation areas and 2030 targets for CARD countries (CARD 2022), sorted by completion percentage

No.	Country	Result	Target/Ha	Ratio	Region
1	Angola	30375	11531	263%	Central
2	Central African Republic	70545	30350	232%	Central
3	Chad	501287	254580	197%	Central

4	Democratic Republic of the Congo	1523243	776000	196%	Central
5	Ghana	709060	372330	190%	Western
6	Burundi	102335	68244	150%	Eastern
7	Malawi	120866	82621	146%	Eastern
8	Uganda	368356	280000	132%	Eastern
9	Cameroon	403379	334764	120%	Central
10	Guinea-Bissau	178277	155046	115%	Western
11	Zambia	83916	80266	105%	Eastern
12	Rwanda	61969	60000	103%	Eastern
13	Togo	194153	193000	101%	Western
14	Benin	215851	242000	89%	Western
15	Gambia	206632	247009	84%	Western
16	Madagascar	1537131	2105690	73%	Eastern
17	Mozambique	415471	570272	73%	Eastern
18	Côte d'Ivoire	727320	1003580	72%	Western
19	Mali	914169	1283970	71%	Western
20	Guinea	1580359	2547881	62%	Western
21	Nigeria	4889668	8523687	57%	Western
22	United Republic of Tanzania	1160821	2200000	53%	Eastern
23	Senegal	384397	775053	50%	Western
24	Ethiopia	155157	327252	47%	Eastern
25	Burkina Faso	273063	627587	44%	Western
26	Sierra Leone	694314	1602103	43%	Western
27	Liberia	135214	326183	41%	Western
28	Sudan	52553	142856	37%	Northern
29	Niger	85573	252507	34%	Western
30	Kenya	59220	222000	27%	Eastern

495
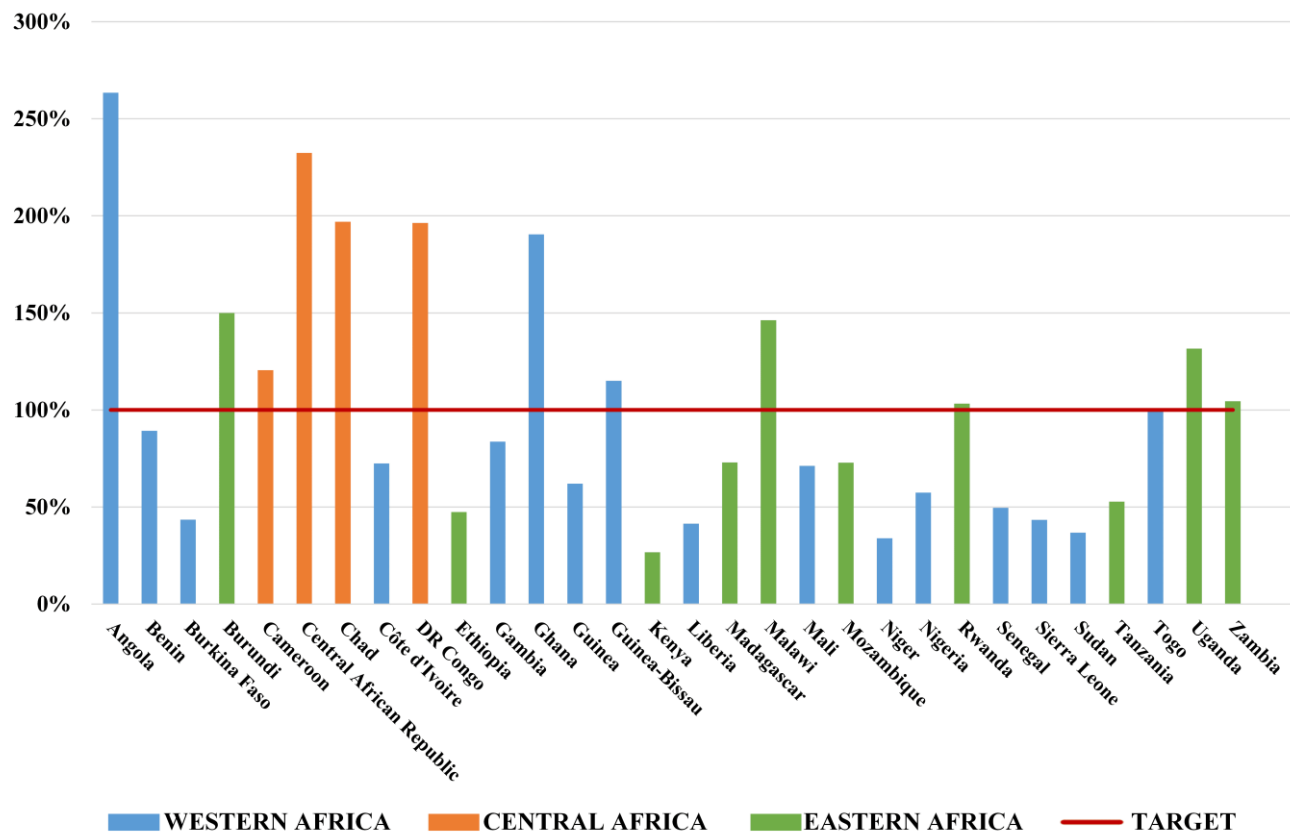
Figure 15. Comparison of current rice planting areas and 2030 targets for CARD countries

6 Data Availability

The 20m Africa Rice Distribution Map of 2023 can be accessed in the Zenodo data set from the following DOI:

500   https://doi.org/10.5281/zenodo.13729353 (Jiang et al., 2024). The spatial reference system of the data set is EPSG:4326(WGS84).

7 Conclusion

This study employs temporal SAR data and optical imagery, combined with object-oriented segmentation, and feature importance guided random forest algorithms, to conduct rice extraction experiments in 34 African countries with annual rice

505   planting areas exceeding 5,000 hectares, achieving 20-meter resolution spatial distribution mapping of rice in Africa for 2023.

The average classification accuracy on the validation set exceeded 85%, and the R² values for linear fitting with existing statistical data all surpassed 0.9, demonstrating the effectiveness of the proposed mapping method.

This study marks the first time a high-resolution rice spatial distribution map has been generated for the entire African continent, offering significant advancements in monitoring rice cultivation patterns in the region. The map provides crucial data support for rice yield estimation, climate resilience assessments, and the development of targeted agricultural policies. Moreover, the insights derived from this research can aid in optimizing resource allocation, enhancing food security, and informing decision-making processes for stakeholders ranging from policymakers to local farmers across Africa.

Author Contributions: Conceptualization, methodology, software, J.J., M.S. and J.G; validation, formal analysis, J.J., and J.G.; investigation, J.J., and H.Z.; resources, data curation, L.X., Y.D., and Y.X.; writing—original draft preparation, J.J., and H.Z.; writing—review and editing, H.Z., L.X., J.G. and L.Z.; visualization, J.J., Y.D., Y.X.; supervision, project administration, H.Z., L.Z., and W.H. All authors have read and agreed to the published version of the manuscript.

Funding: The research was supported by the National Natural Science Foundation of China (T2261129473), and the National Key R&D Program of China (grant numbers 2023YFB3906201).

Acknowledgments: The authors acknowledge the support of data and computational power provided by the Google Earth Engine platform.

Conflicts of Interest: The authors declare no conflict of interest.

References

Achanta, R. and Susstrunk, S.: Superpixels and polygons using simple non-iterative clustering, Proceedings of the IEEE conference on computer vision and pattern recognition, 4651-4660,

AfricaRice: Africa Rice Center (AfricaRice). 2023. Transformation of Rice-based Agri-food Systems for Food and Nutrition Security in Africa: 2030 rice research and innovation strategy for Africa. Abidjan, Côte d'Ivoire: vi+58 pp., 2023.

Ajala, A. and Gana, A.: Analysis of challenges facing rice processing in Nigeria, Journal of food processing, 2015, 893673, 2015.

Arouna, A., Fatognon, I. A., Saito, K., and Futakuchi, K.: Moving toward rice self-sufficiency in sub-Saharan Africa by 2030: Lessons learned from 10 years of the Coalition for African Rice Development, World Development Perspectives, 21, 100291, https://doi.org/10.1016/j.wdp.2021.100291, 2021.

Avcı, C., Budak, M., Yağmur, N., and Balçık, F.: Comparison between random forest and support vector machine algorithms for LULC classification, International Journal of Engineering and Geosciences, 8, 1-10, 2023.

Balasubramanian, V., Sie, M., Hijmans, R. J., and Otsuka, K.: Increasing Rice Production in Sub-Saharan Africa: Challenges and Opportunities, in: Advances in Agronomy, edited by: Sparks, D. L., Academic Press, 55-133, https://doi.org/10.1016/S0065-2113(06)94002-4, 2007.

Barro, M., Kassankogno, A. I., Wonni, I., Sereme, D., Somda, I., Kabore, H. K., Bena, G., Brugidou, C., Tharreau, D., and Tollenaere, C.: Spatiotemporal Survey of Multiple Rice Diseases in Irrigated Areas Compared to Rainfed Lowlands in the Western Burkina Faso, Plant Dis, 105, 3889-3899, 10.1094/PDIS-03-21-0579-RE, 2021.

Bhogapurapu, N., Dey, S., Mandal, D., Bhattacharya, A., Karthikeyan, L., McNairn, H., and Rao, Y.: Soil moisture retrieval over croplands using dual-pol L-band GRD SAR data, Remote Sensing of Environment, 271, 112900, 2022.

COALITION for African Rice Development: COUNTRIES: https://riceforafrica.net/, last

Chang, J. G., Shoshany, M., and Oh, Y.: Polarimetric radar vegetation index for biomass estimation in desert fringe ecosystems,
545   IEEE Transactions on Geoscience and Remote Sensing, 56, 7102-7108, 2018.

Charbonneau, F., Trudel, M., and Fernandes, R.: Use of Dual Polarization and Multi-Incidence SAR for soil permeability mapping, Proceedings of the 2005 advanced synthetic aperture radar (ASAR) workshop, St-Hubert, QC, Canada, 15-17,

Chhabra, A., Rüdiger, C., Yebra, M., Jagdhuber, T., and Hilton, J.: RADAR-Vegetation Structural Perpendicular Index (R-VSPI) for the Quantification of Wildfire Impact and Post-Fire Vegetation Recovery, Remote Sensing, 14, 3132, 2022.

550   de Lima, I. P., Jorge, R. G., and de Lima, J. L. P.: Remote sensing monitoring of rice fields: Towards assessing water saving irrigation management practices, Frontiers in Remote Sensing, 2, 762093, 2021.

Diuk-Wasser, M. A., Toure, M. B., Dolo, G., Bagayoko, M., Sogoba, N., Sissoko, I., Traoré, S. F., and Taylor, C. E.: Effect of rice cultivation patterns on malaria vector abundance in rice-growing villages in Mali, The American journal of tropical medicine and hygiene, 76, 869, 2007.

555   FAOSTAT: Crops and livestock products: https://www.fao.org/faostat/en/#data/QCL, last

FAO: World Food and Agriculture – Statistical Yearbook 2023, 10.4060/cc8166en, 2023.

Livelihoods Zone Map and Descriptions for South Sudan, last

Field, C. B. and Barros, V. R.: Climate change 2014–Impacts, adaptation and vulnerability: Regional aspects, Cambridge University Press2014.

560   Frolking, S., Wisser, D., Grogan, D., Proussevitch, A., and Glidden, S.: GAEZ+_2015 Crop Harvest Area (V4), Harvard Dataverse [dataset], doi:10.7910/DVN/KAGRFI, 2020.

Ginting, F. I., Rudiyanto, R., Fatchurahman, Mohd Shah, R., Che Soh, N., Giap, S. G. E., Fiantis, D., Setiawan, B. I., Schiller, S., and Davitt, A.: SEA-Rice-Ci10: High-resolution Mapping of Rice Cropping Intensity and Harvested Area Across Southeast Asia using the Integration of Sentinel-1 and Sentinel-2 Data, Earth System Science Data Discussions, 2024, 1-49, 2024.

565   Gorelick, N., Hancher, M., Dixon, M., Ilyushchenko, S., Thau, D., and Moore, R.: Google Earth Engine: Planetary-scale geospatial analysis for everyone, Remote sensing of Environment, 202, 18-27, 2017.

Guan, X., Huang, C., Liu, G., Meng, X., and Liu, Q.: Mapping Rice Cropping Systems in Vietnam Using an NDVI-Based Time-Series Similarity Measurement Based on DTW Distance, Remote Sensing, 8, 19, 2016.

Guo, Y., Jia, X., Paull, D., and Benediktsson, J. A.: Nomination-favoured opinion pool for optical-SAR-synergistic rice
570   mapping in face of weakened flooding signals, ISPRS Journal of Photogrammetry and Remote Sensing, 155, 187-205, 2019.

Han, J., Zhang, Z., Luo, Y., Cao, J., Zhang, L., Cheng, F., Zhuang, H., Zhang, J., and Tao, F.: NESEA-Rice10: high-resolution annual paddy rice maps for Northeast and Southeast Asia from 2017 to 2019, Earth System Science Data, 13, 5969-5986, 2021.

Hussain, S., Huang, J., Huang, J., Ahmad, S., Nanda, S., Anwar, S., Shakoor, A., Zhu, C., Zhu, L., and Cao, X.: Rice production under climate change: adaptations and mitigating strategies, Environment, climate, plant and vegetation growth, 659-686, 2020.

575   International Food Policy Research, I.: Spatially-Disaggregated Crop Production Statistics Data in Africa South of the Sahara for 2017 (V3), Harvard Dataverse [dataset], doi:10.7910/DVN/FSSKBW, 2020.

Jiang, J., Zhang, H., Ge, J., Zuo, L., Xu, L., Song, M., Ding, Y., Xie, Y., and Huang, W.: 20m Africa rice distribution map in 2023 [dataset], https://doi.org/10.5281/zenodo.13729353 [dataset], https://doi.org/10.5281/zenodo.13729353, 2024.

Kajisa, K. and Vu, T. T.: The importance of farm management training for the African rice Green Revolution: Experimental
580   evidence from rainfed lowland areas in Mozambique, Food Policy, 114, 102401, 2023.

Kuenzer, C. and Knauer, K.: Remote sensing of rice crop areas, International Journal of Remote Sensing, 34, 2101-2139, 2013.

Kwesiga, J., Grotelüschen, K., Neuhoff, D., Senthilkumar, K., Döring, T. F., and Becker, M.: Site and management effects on grain yield and yield variability of rainfed lowland rice in the Kilombero Floodplain of Tanzania, Agronomy, 9, 632, 2019.

Laborte, A. G., Gutierrez, M. A., Balanza, J. G., Saito, K., Zwart, S. J., Boschetti, M., Murty, M. V. R., Villano, L., Aunario,
585   J. K., Reinke, R., Koo, J., Hijmans, R. J., and Nelson, A.: RiceAtlas, a spatial database of global rice calendars and production, Scientific Data, 4, 10.1038/sdata.2017.74, 2017.

Li, J. and Wang, S.: Using SAR-Derived Vegetation Descriptors in a Water Cloud Model to Improve Soil Moisture Retrieval, Remote Sensing, 10, 1370, 2018.

Liang, S., Li, Y., Zheng, Z., Cui, C., and Zhao, J.: Development Suggestions and Cultivation Performance of Chinese Hybrid
590   Rice Varieties in Chad, 湖北农业科学, 56, 1422-1426, 10.14088/j.cnki.issn0439-8114.2017.08.006, 2017.

Liu, X., Zhai, H., Shen, Y., Lou, B., Jiang, C., Li, T., Hussain, S. B., and Shen, G.: Large-scale crop mapping from multisource remote sensing images in google earth engine, IEEE Journal of Selected Topics in Applied Earth Observations and Remote Sensing, 13, 414-427, 2020.

Liu, X., Zheng, J., Yu, L., Hao, P., Chen, B., Xin, Q., Fu, H., and Gong, P.: Annual dynamic dataset of global cropping intensity from 2001 to 2019, Scientific Data, 8, 283, 10.1038/s41597-021-01065-9, 2021.

Loko, Y. L. E., Gbemavo, C. D. S. J., Djedatin, G., Ewedje, E.-E., Orobiyi, A., Toffa, J., Tchakpa, C., Sedah, P., and Sabot, F.: Characterization of rice farming systems, production constraints and determinants of adoption of improved varieties by smallholder farmers of the Republic of Benin, Scientific Reports, 12, 3959, 10.1038/s41598-022-07946-2, 2022.

Luo, K., Lu, L., Xie, Y., Chen, F., Yin, F., and Li, Q.: Crop type mapping in the central part of the North China Plain using Sentinel-2 time series and machine learning, Computers and Electronics in Agriculture, 205, 107577, 2023.

Mathieu, R.: Mapping of Rice Areas in Egypt using SAR Imagery, 2022.

Menge, D. M., Musila, R. N., Kagito, S., Bii, L., Gichuki, J., Gichuhi, E., Kundu, C. A., Murori, R., Ismail, A., and Panchbhai, A.: Using principal component analysis to assess soil chemical properties in the mwea irrigation Scheme, Kenya: Implications for rice agronomic management, International Journal of Plant & Soil Science, 36, 106-126, 2024.

Mwakyusa, L., Dixit, S., Herzog, M., Heredia, M. C., Madege, R. R., and Kilasi, N. L.: Flood-tolerant rice for enhanced production and livelihood of smallholder farmers of Africa, Frontiers in Sustainable Food Systems, 7, 1244460, 2023.

Ogisi, O. D. and Begho, T.: Adoption of climate-smart agricultural practices in sub-Saharan Africa: A review of the progress, barriers, gender differences and recommendations, Farming System, 1, 100019, https://doi.org/10.1016/j.farsys.2023.100019, 2023.

Panda, D. and Barik, J.: Flooding tolerance in rice: Focus on mechanisms and approaches, Rice Science, 28, 43-57, 2021.

Qiu, B., Li, W., Tang, Z., Chen, C., and Qi, W.: Mapping paddy rice areas based on vegetation phenology and surface moisture conditions, Ecological Indicators, 56, 79-86, 2015.

Saad El Imanni, H., El Harti, A., Hssaisoune, M., Velastegui-Montoya, A., Elbouzidi, A., Addi, M., El Iysaouy, L., and El Hachimi, J.: Rapid and automated approach for early crop mapping using Sentinel-1 and Sentinel-2 on Google earth engine; a case of a highly heterogeneous and fragmented agricultural region, Journal of Imaging, 8, 316, 2022.

Seck, P. A., Diagne, A., Mohanty, S., and Wopereis, M. C.: Crops that feed the world 7: Rice, Food security, 4, 7-24, 2012.

Shen, R., Pan, B., Peng, Q., Dong, J., Chen, X., Zhang, X., Ye, T., Huang, J., and Yuan, W.: High-resolution distribution maps of single-season rice in China from 2017 to 2022, Earth System Science Data Discussions, 2023, 1-27, 2023.

Singh, R. K., Rizvi, J., Behera, M. D., and Biradar, C.: Automated crop type mapping using time-weighted dynamic time warping-A basis to derive inputs for enhanced food and Nutritional Security, Current Research in Environmental Sustainability, 3, 100032, 2021.

Sun, C., Zhang, H., Xu, L., Ge, J., Jiang, J., Song, M., and Wang, C.: Rice yield prediction using radar vegetation indices from Sentinel-1 data and multiscale one-dimensional convolutional long-and short-term memory network model, Journal of Applied Remote Sensing, 18, 024505-024505, 2024.

Sun, C., Zhang, H., Xu, L., Ge, J., Jiang, J., Zuo, L., and Wang, C.: Twenty-meter annual paddy rice area map for mainland Southeast Asia using Sentinel-1 synthetic-aperture-radar data, Earth System Science Data, 15, 1501-1520, 10.5194/essd-15-1501-2023, 2023.

Tang, F. H., Nguyen, T. H., Conchedda, G., Casse, L., Tubiello, F. N., and Maggi, F.: CROPGRIDS: A global geo-referenced dataset of 173 crops circa 2020, Earth System Science Data Discussions, 2023, 1-22, 2023.

Tassi, A. and Vizzari, M.: Object-oriented lulc classification in google earth engine combining snic, glcm, and machine learning algorithms, Remote Sensing, 12, 3776, 2020.

Tian, G., Li, H., Feng, X., Jiang, Q., Li, N., Guo, Z., Zhao, J., and Yang, H.: An automatic method for rice mapping in Taishan, China using Sentinel-1A Time-series images, Remote Sensing Letters, 15, 99-109, 2024.

Foreign Agricultural Service: https://ipad.fas.usda.gov/countrysummary, last

Voahanyinirina, R. and Elie, R.: Effects of planting location and storage time on lipids and fatty acids contents of some Madagascan rice varieties, African Journal of Agriculture Research, 2, 349-355, 2007.

Waleed, M., Mubeen, M., Ahmad, A., Habib-ur-Rahman, M., Amin, A., Farid, H. U., Hussain, S., Ali, M., Qaisrani, S. A., and Nasim, W.: Evaluating the efficiency of coarser to finer resolution multispectral satellites in mapping paddy rice fields using GEE implementation, Scientific Reports, 12, 13210, 2022.

Wang, G., Meng, D., Chen, R., Yang, G., Wang, L., Jin, H., Ge, X., and Feng, H.: Automatic Rice Early-Season Mapping Based on Simple Non-Iterative Clustering and Multi-Source Remote Sensing Images, Remote Sensing, 16, 277, 2024.

Wang, Y., Zang, S., and Tian, Y.: Mapping paddy rice with the random forest algorithm using MODIS and SMAP time series, Chaos, Solitons & Fractals, 140, 110116, 2020.

Wei, J., Cui, Y., Luo, W., and Luo, Y.: Mapping paddy rice distribution and cropping intensity in China from 2014 to 2019 with landsat images, effective flood signals, and google earth engine, Remote Sensing, 14, 759, 2022.

Wu, H., Zhang, J., Zhang, Z., Han, J., Cao, J., Zhang, L., Luo, Y., Mei, Q., Xu, J., and Tao, F.: AsiaRiceYield4km: seasonal rice yield in Asia from 1995 to 2015, Earth System Science Data Discussions, 2022, 1-30, 2022.

Yamamoto, Y., Tsujimoto, Y., Fujihara, Y., Sakagami, J.-i., Ochi, S., and Fosu, M.: Assessing the probability of land submergence for lowland rice cultivation in Africa using satellite imagery and geospatial data, Environment, development and sustainability, 14, 955-971, 2012.

You, N., Dong, J., Huang, J., Du, G., Zhang, G., He, Y., Yang, T., Di, Y., and Xiao, X.: The 10-m crop type maps in Northeast China during 2017-2019, Sci Data, 8, 41, 10.1038/s41597-021-00827-9, 2021a.

You, N., Dong, J., Huang, J., Du, G., Zhang, G., He, Y., Yang, T., Di, Y., and Xiao, X.: The 10-m crop type maps in Northeast China during 2017–2019, Scientific data, 8, 41, 2021b.

Yu, Q., You, L., Wood-Sichra, U., Ru, Y., Joglekar, A. K., Fritz, S., Xiong, W., Lu, M., Wu, W., and Yang, P.: A cultivated planet in 2010–Part 2: The global gridded agricultural-production maps, Earth System Science Data, 12, 3545-3572, 2020.

Yuan, S., Saito, K., van Oort, P. A. J., van Ittersum, M. K., Peng, S., and Grassini, P.: Intensifying rice production to reduce imports and land conversion in Africa, Nature Communications, 15, 835, 10.1038/s41467-024-44950-8, 2024.

Zhan, P., Zhu, W., and Li, N.: An automated rice mapping method based on flooding signals in synthetic aperture radar time series, Remote Sensing of Environment, 252, 112112, 2021.

Zhang, B., Liu, X., Liu, M., and Meng, Y.: Detection of Rice Phenological Variations under Heavy Metal Stress by Means of Blended Landsat and MODIS Image Time Series, Remote Sensing, 11, 13, 2019.

Zhang, M., Wu, B., Zeng, H., He, G., Liu, C., Tao, S., Zhang, Q., Nabil, M., Tian, F., and Bofana, J.: GCI30: A global dataset of 30-m cropping intensity using multisource remote sensing imagery, Earth System Science Data Discussions, 2021, 1-22, 2021.

Zhang, W., Liu, H., Wu, W., Zhan, L., and Wei, J.: Mapping rice paddy based on machine learning with Sentinel-2 multi-temporal data: Model comparison and transferability, Remote Sensing, 12, 1620, 2020.

Zhang, X., Shen, R., Zhu, X., Pan, B., Fu, Y., Zheng, Y., Chen, X., Peng, Q., and Yuan, W.: Sample-free automated mapping of double-season rice in China using Sentinel-1 SAR imagery, Frontiers in Environmental Science, 11, 10.3389/fenvs.2023.1207882, 2023.

Zhu, A.-X., Zhao, F.-H., Pan, H.-B., and Liu, J.-Z.: Mapping rice paddy distribution using remote sensing by coupling deep learning with phenological characteristics, Remote sensing, 13, 1360, 2021.

Zoungrana, L. E., Barbouchi, M., Toukabri, W., Babasy, M. O., Khatra, N. B., Annabi, M., and Bahri, H.: Sentinel SAR-optical fusion for improving in-season wheat crop mapping at a large scale using machine learning and the Google Earth engine platform, Applied Geomatics, 16, 147-160, 2024.